British Geological Survey

A Magnetotelluric experiment around St. Austell, Cornwall

Multi-hazards and resilience Programme

Open Report OR/23/031

BRITISH GEOLOGICAL SURVEY

MULTI-HAZARDS AND RESILIENCE PROGRAMME

OPEN REPORT OR/23/031

A Magnetotelluric Experiment around St. Austell, Cornwall

J. Huebert

Contributor/editor

C.D. Beggan

Keywords

Geothermal, magnetotellurics, Cornwall, St Austell granite.

Front cover

Remote magnetotelluric installation at a site in Bodmin Moor, Cornwall.

Bibliographical reference

HUEBERT, J.2023. A Magnetotelluric Experiment around St. Austell, Cornwall. *British Geological Survey Open Report*, OR/23/031. 48pp.

Lyell Centre, Edinburgh British Geological Survey 2023

BRITISH GEOLOGICAL SURVEY

Our range of publications is available from BGS shops at Nottingham, London and Cardiff (Welsh publications only). Shop online at shop.bgs.ac.uk.

We publish an annual catalogue of our maps and other publications; this catalogue is available online or from BGS shops.

The British Geological Survey carries out the geological survey of Great Britain and Northern Ireland (the latter as an agency service for the government of Northern Ireland), and of the surrounding continental shelf, as well as basic research projects. It also undertakes programmes of technical assistance in geology in low- to middle-income countries.

The British Geological Survey is a component body of UK Research and Innovation.

British Geological Survey offices

Nicker Hill, Keyworth, Nottingham NG12 5GG
Tel 0115 936 3100

BGS Central Enquiries Desk
Tel 0115 936 3143
email enquiries@bgs.ac.uk

BGS Sales
Tel 0115 936 3241
email sales@bgs.ac.uk

The Lyell Centre, Research Avenue South, Edinburgh EH14 4AP
Tel 0131 667 1000

Natural History Museum, Cromwell Road, London SW7 5BD
Tel 020 7589 4090
Tel 020 7942 5344/45
email bgslondonstaff@bgs.ac.uk

Cardiff University, Main Building, Park Place, Cardiff CF10 3AT
Tel 029 2167 4280

Maclean Building, Crowmarsh Gifford, Wallingford OX10 8BB
Tel 01491 838800

Geological Survey of Northern Ireland, Department for the Economy, Dundonald House, Upper Newtownards Road, Ballymiscaw, Belfast, BT4 3SB
Tel 0289 038 8462
www2.bgs.ac.uk/gsni/

Natural Environment Research Council, Polaris House, North Star Avenue, Swindon SN2 1EU
Tel 01793 411500
Fax 01793 411501
www.nerc.ac.uk

UK Research and Innovation, Polaris House, Swindon SN2 1FL
Tel 01793 444000
www.ukri.org

Website www.bgs.ac.uk
Shop online at shop.bgs.ac.uk

Foreword

This report is the published product of a study by the British Geological Survey (BGS). The presented work was jointly funded by the BGS' internal Innovation Flexible Fund (IFF) and under contract to Eden Geothermal Ltd (project number NEE9148R) to investigate the potential to use the magnetotelluric deep sounding technique for the characterization of geothermal reservoirs at depth in semi-urban environments. Developments in instrumentation, software and computational processing over the past 10 years have made it possible to conduct this type of study in areas where noise sources from infrastructure can be expected.

Acknowledgements

We thank Eden Geothermal Ltd (EGL) for their interest in our work and for their support, especially with initial site scouting and making contact with local landowners. We thank Deep Digital Cornwall for supplying extra funding to support the field campaign.

We wish to thank the landowners for granting access to field locations. Special thanks go to Colin Hogg from Dublin Institute for Advanced Studies (DIAS) for training and technical support during the magnetotelluric instrument loan. We thank University of Edinburgh's Aideliz Montiel Alvarez for assistance during the field campaign. BGS staff Eliot Eaton, Adam Collins and Dave Morgan are thanked for making the data collection possible and persevering during challenging weather conditions and tight schedules. Christopher Rochelle is thanked for his support during the planning of this project and for facilitating the collaboration with EGL.

Contents

FIGURES

Summary

In this BGS Open Report we describe the results of a pilot study assessing the potential of the magnetotelluric (MT) method to characterize geothermal reservoirs at depth when the target site is in a semi-urban environment. During an MT survey, the natural variations of the electromagnetic field of the Earth are measured at the field site for time windows of a few hours up to a couple of days. As a passive geophysical technique, the data quality is dependent on the *in-situ* electromagnetic noise levels. The noise come from technological infrastructure that dominates the landscape of modern Britain such as power lines, high voltage transformers, electric fences, radio towers, electrified railways and gas pipeline protection systems. In the absence of artificial noise, the MT method can sample the shallow and deep subsurface of the Earth down to the lower crust and mantle depending on the frequency of the measured signal. MT images the bulk electrical conductivity of the rocks and can therefore indicate the presence of fluids at depth. For deep geothermal exploration, MT has been identified as one of the few geophysical techniques able to help characterise geothermal host rocks and zones of enhanced permeability and porosity which are necessary for the fluid circulation of an enhanced geothermal system.

Deep geothermal exploration in the UK has, so far, been limited to the granites of Cornwall which are known to have relatively high heat flow. Along with a strong legacy knowledge of the geology of the subsurface these have encouraged two deep geothermal drill projects. At the Eden Geothermal site close to the Eden Project in St Austell, a 5,277 m deep borehole was drilled into the St Austell granite to intersect with a known geologic fault zone, the NNW-SSE striking Great Cross-Course (GXC) Fault, where the circulation of geothermal fluids in a closed loop system was deemed possible. The drilling was partly sponsored by the European Regional Development Fund and designed as both a research facility and to provide green energy to the Eden Project and adjacent businesses. The position and extent of the fault zone at depth was not known and previous geophysical surveys had been limited to very shallow depths. Seismic monitoring has been an ongoing component of the drilling and ensuing pump testing.

During a 10-day field campaign in March 2023 a team from BGS were able to collect broadband MT data at 30 sites in the St Austell area and one remote site in Bodmin Moor to help improve data quality through remote referencing time-series processing techniques. Data collected very close to the drill site and at some locations close to town centres have low quality, but overall data quality was sufficient to allow modelling of the electrical properties at depth. The derived MT impedance tensors were used to construct a 3D model of the area which has low spatial resolution but clearly shows that MT data can image the local geology at depth. The St Austell granite is characterized by high resistivities, whereas the onshore sediments and metasediments surrounding the intrusion have lower resistivities. Some vertical structures of lower resistivity within the granite were identified and are carefully investigated.

Overall, the use of the MT method for the characterisation of geothermal reservoirs in granitic bodies is confirmed in this study. Further data collection and modelling is recommended to improve the spatial resolution at depth.

1 Introduction

1.1 GEOTHERMAL ENERGY IN THE UK

Increasing geothermal energy production is one of the UK's Net Zero strategies. In order to harvest this low carbon heat source, it is necessary to characterise the geologic formations with increased heat flow at depth. Geophysical methods are a very cost-effective way of studying this from the subsurface and allow de-risking of geothermal drilling. In recent years, the revision of heat flow maps based on airborne geophysics (see Fig. 1) has identified the Cornish granite intrusions as zones of increased heat flow and potential sites for geothermal exploitation [*Beamish and Busby*, 2016]. The revised estimates for temperatures at depth (e.g., 221°C at 5 km depth at the St Austell and 200 °C at 5 km depth in the Carnmenellis granites) encouraged new geothermal projects to go ahead. At United Downs in Redruth, drilling and geothermal heat production is, at present, the most advanced in the UK [*Paulillo et al.*, 2020; *Reinecker et al.*, 2021]. A second site for geothermal deep drilling was chosen close to the Eden Project in St Austell.

Magnetotelluric (MT) measurements have been widely used to image the subsurface for geothermal exploration and heat flow modelling in high enthalpy ('hot') regions like Iceland and Ethiopia but rarely in lower enthalpy countries like the UK. Recently, MT has been used to assess the geothermal potential in Ireland [*Vozar et al.*, 2020].

In this project we collected and analysed MT data in a semi-urban area (Cornwall) to investigate if it is possible to make measurements with sufficiently high data quality to characterise geothermal reservoirs at depth.

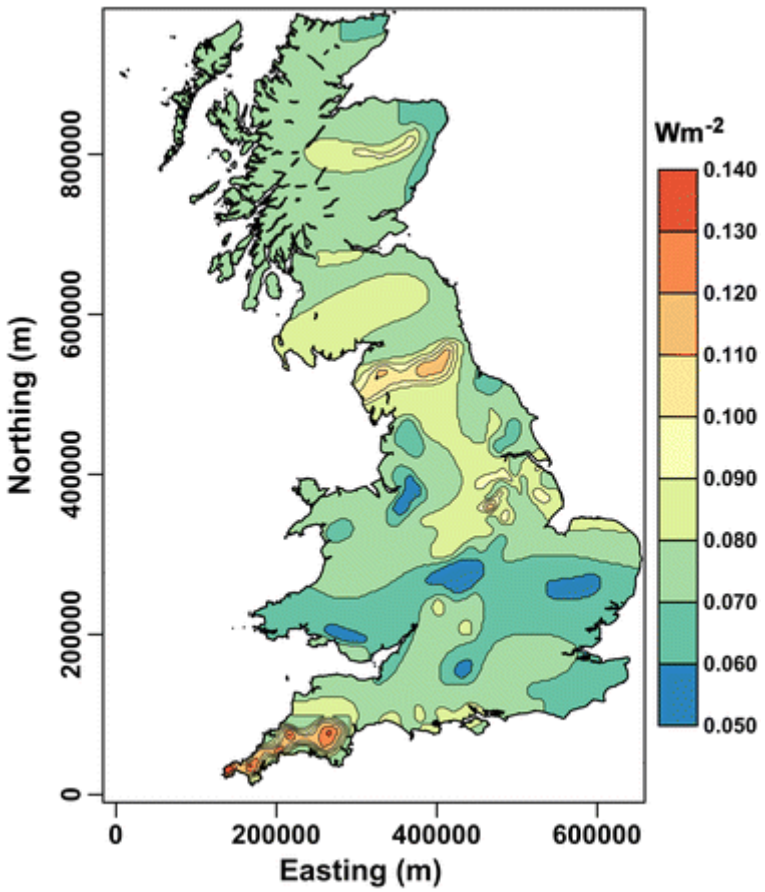

Figure 1: Surface heat flow map for Great Britain from [*Busby and Terrington*, 2017].

1.2 MAGNETOTELLURICS FOR GEOTHERMAL EXPLORATION

Magnetotellurics (MT) is a deep-sounding geophysical imaging technique that uses the wide-band natural variations in the electromagnetic field of the Earth to infer the electrical conductivity of the subsurface using the principles of electromagnetic induction. MT has been widely used to image subsurface features relevant to geothermal exploration, especially in high enthalpy regions like Iceland and Ethiopia. Work has been done to also study lower enthalpy reservoirs in Germany, Italy and Ireland with MT data [*Munoz*, 2014; *Tripaldi*, 2020; *Vozar et al.*, 2020].

In the UK, modern MT investigations have been sparse. The greatest challenge to the method is electromagnetic noise from man-made infrastructure. Broadband MT data were previously collected near the Carnmemellis granite in the early 1990s [*Jones*, 1992] during the Hot Dry Rock geothermal programme. At that time, data quality was low and computational methods required to analyse this data in three dimensions were not very advanced. Since then, there have been huge improvements in magnetotelluric instrumentation and also in data analysis and processing tools. We initiated a pilot MT survey centred around the southern part of the St Austell Granite (including the Eden Geothermal site) as a good location to test the feasibility of using MT in a semi-urban environment by employing modern instrumentation and new computational methods.

The regional geology is dominated by the granitic St Austell intrusion (see Fig 2). Zones of increased fracturing and higher permeability and porosity are the targets for geothermal exploration because they can provide pathways for fluid circulation which is essential for heat production. Dry granitic rocks themselves are highly resistive due to the lack of charge carriers (i.e., free electrons) in the mineral assemblage. On the contrary, when the rock is deformed and fluids circulate, this greatly increasing the bulk electrical conductivity. These sharp and potentially steeply dipping contrasts should be detected by MT. The Great Cross-Course Fault within the St. Austell granite has been the target of the geothermal drilling.

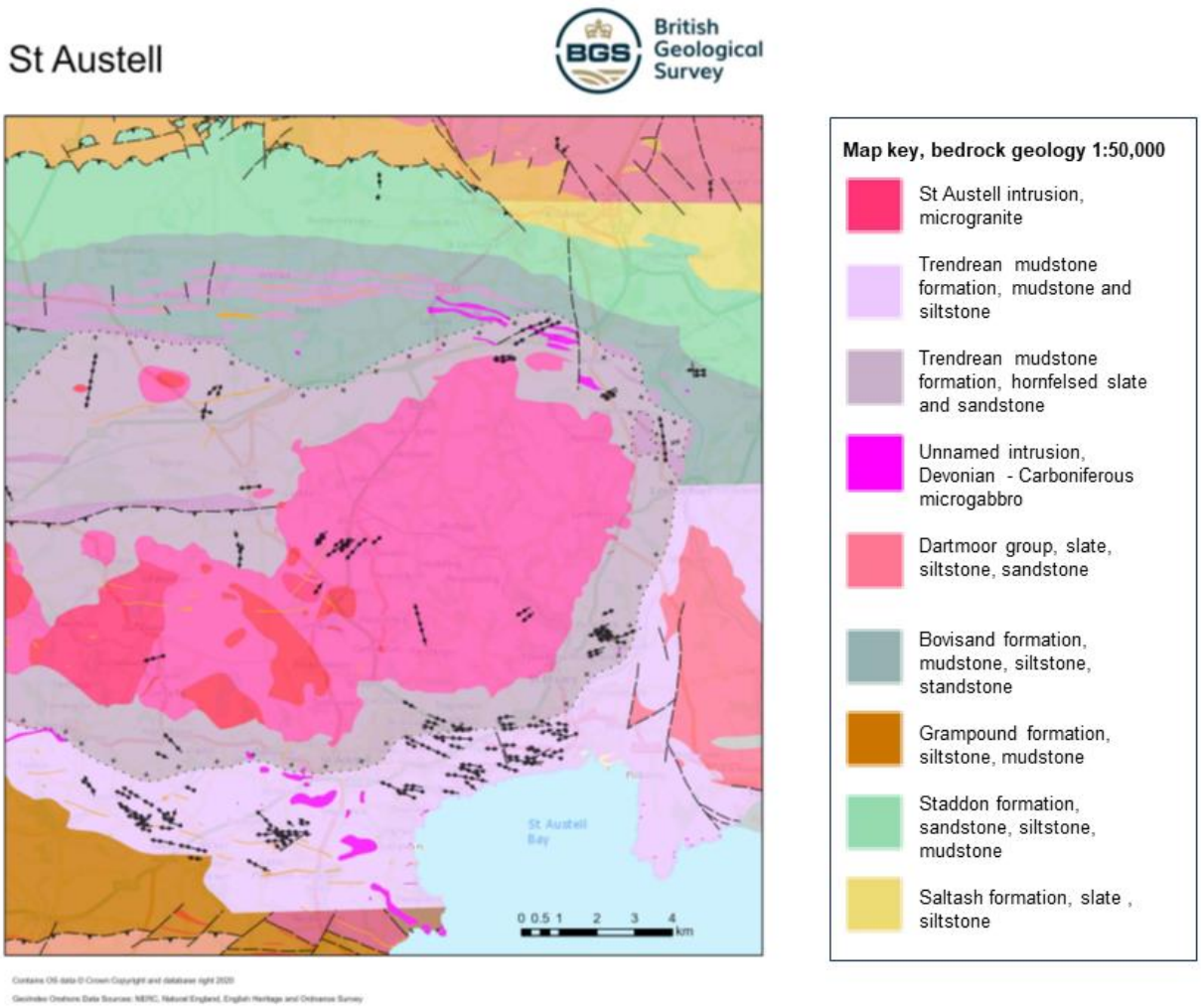

Figure 2: Bedrock geology and linear features in the St Austell area. Plotted using BGS GeoIndex Onshore data. BGS © UKRI. All Rights Reserved.

The overall aims of this study were:

1. to trial the MT method in a suburban environment to check if data quality is satisfactory;

2. to undertake preliminary three-dimensional modelling of the collected data to see if there are conductive features at depth which might be associated with known fault structures and zones of increased permeability and potentially fluid-bearing.

1.3 THE EDEN GEOTHERMAL DRILL SITE

Figure 3: Geothermal drill site at the Eden Project, Cornwall, visited during the field campaign. The site was being prepared for pump tests with a new heat exchanger at the time of the visit.

The Eden Geothermal Ltd (EGL) drill site is located on the compound of the Eden Project, a world-famous educational charity, where an old china clay pit has been transformed into an ecological visitor attraction. Several large biomes house plants from different climate zones around the world, requiring constant heating. Use of heat from geothermal fluids below the site was a motivating factor for developing the geothermal potential of the area.

Drilling of the first deep borehole was completed in 2021 and serves as a unique in-situ research facility for geothermal exploration in the UK (see Fig. 3). The borehole reaches a depth of 4,871 m below surface and has a total length of 5,277 m, most of which has been stabilised with steel casing. Well and pump tests have been performed to study possible flow rates. A heat exchanger was installed in early 2023. In a planned second phase, not yet initiated, a second borehole will be placed so that fluid circulation in the fault zone at depth would be optimized within the local stress regime.

In addition to the industrial and mining activity around the drill site, there are a variety of other construction and farming activities in the area that produce unwanted electromagnetic noise in the MT frequency range.

2 MT data collection in the St Austell area

The magnetotelluric (MT) method is a deep-sounding geophysical technique that uses the principles of electromagnetic induction to study the interior of the earth [*Chave*, 2012]. By simultaneously recording the variations in the natural magnetic and electric field on the surface of the Earth it is possible to derive models of underlying electrical conductivity. In practice, a magnetic sensor (for the broadband frequency range, three induction coil magnetometers are used) samples the magnetic field in cartesian coordinates (x for north-south, y for east-west and z for the vertical field component). The horizontal electric field is measured with two dipoles using non-polarisable electrodes to avoid the influence of geochemical reactions around the probes.

2.1 THE MT IMPEDANCE TENSOR

The recorded time series of the electric and magnetic field are filtered and transformed into frequency spectra which are then used to compute the *impedance tensor*, denoted **Z**.

The impedance tensor is defined in the frequency domain (with $\omega=2\pi/f$) and relates the variation of the magnetic field (**B**) to that of the electric field (**E**):

$$\mathbf{E}(\omega) = \frac{1}{\mu_0}\mathbf{Z}(\omega) \cdot \boldsymbol{B}(\omega)$$

where μ_0 is the permeability of free space. The **Z** tensor is frequency-dependent and has four complex components Zxx, Zxy, Zyx, Zyy:

$$\mathbf{Z} = \begin{pmatrix} Zxx & Zxy \\ Zyx & Zyy \end{pmatrix}$$

The off-diagonal components Zxy and Zyx are typically much larger than the diagonal ones and are therefore referred to as the main components of the impedance tensor. **Z** is often displayed as apparent resistivity with respect to frequency, ρ_a, a measure for the amplitude and the true resistivity if the subsurface is homogeneous:

$$\rho_{a_{ij}}(\omega) = \frac{1}{\mu_0 \omega} \left| Z_{ij}(\omega) \right|^2$$

and phase curves for each component

$$\Phi_{ij} = \tan^{-1}\left(\frac{Im\{Z_{ij}\}}{Re\{Z_{ij}\}}\right)$$

These allow for a quick visual inspection of the magnitude and changes in conductivity in the subsurface with depth (see Fig. 7).

2.2 THE FIELD CAMPAIGN OF MARCH 2023

During March 2023, BGS staff collected broadband magnetotelluric data at 30 site locations in the St Austell area. For the survey layout we chose a dual approach, firstly to collect data in the wider area to gain an insight into data quality and the potential to derive an initial 3D model of the area, and secondly a denser sampling along a profile striking 50° NE-SW that perpendicularly traverses the Great Cross-Course Fault (see Fig. 4).

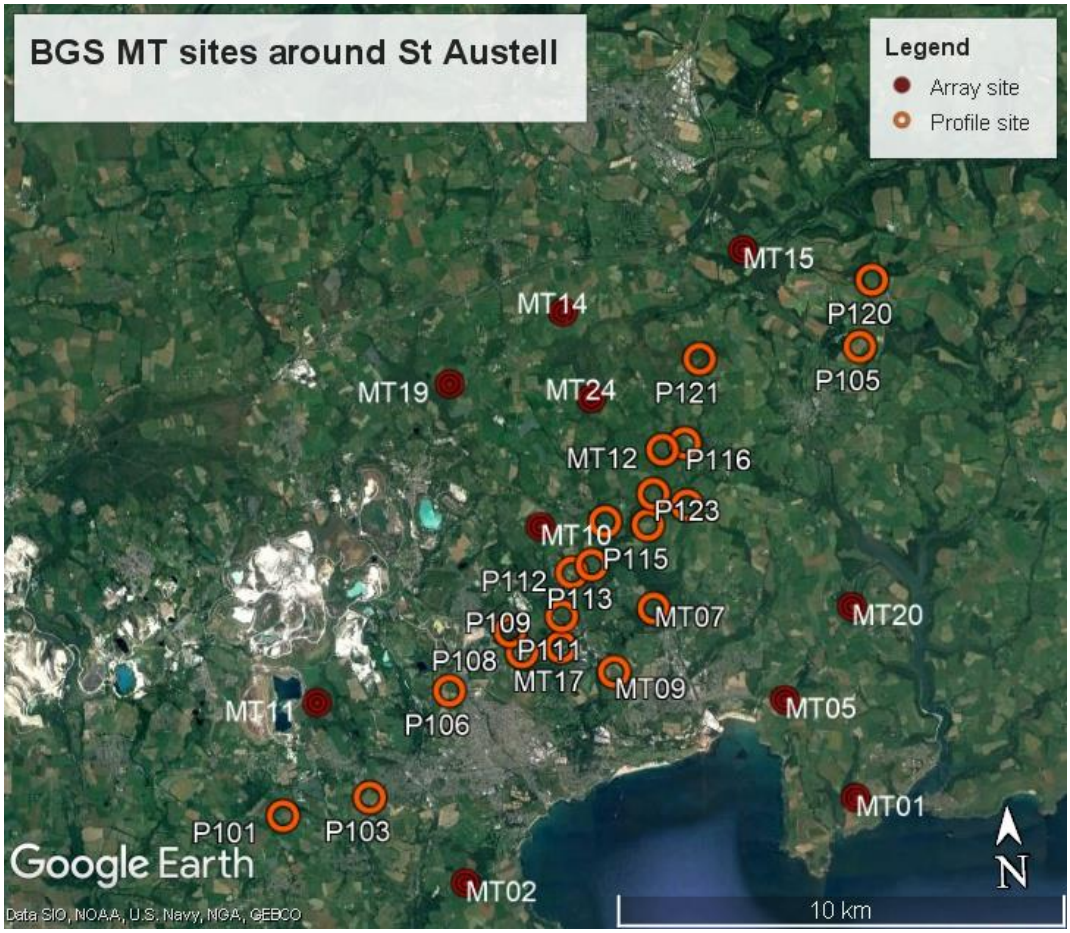

Figure 4 Location of Magnetotelluric sites around St Austell on satellite image. Orange circles indicate sites along a profile crossing the Great Cross-Course Fault and the data are owned by Eden Geothermal Ltd. Red dots are sites for a wider array, data are owned by BGS © UKRI. Background image taken from Google Earth.

Eden Geothermal Ltd (EGL) initiated the contact with local landowners of the prospective locations. As site characteristics, we required at a minimum:

- Open area for the centre of the installation, not in close proximity to trees (<20m away). For a schematic of the site layout see Fig. 5.
- Permission to dig holes (around 50 cm in diameter, up to 1.5 m deep) for the three magnetic induction coil and five electrode (electric field) sensors.
- Vehicle access to within 100 m of the site. This may be off-road, but if so then it would preferably be less than 1 km from a metalled road.
- No livestock (sheep/cows/horses) to be present in the field at the time
- Low electromagnetic environment (e.g. 10 km from a train line, >300 m main road, >1500 m transformers and >500m buildings) where possible.
- Secure access to the land and away from public rights of way to avoid physical disturbance.
- Low physical gradient and well drained soil.
- More than 1 m soil depth so that the soil can be used as insulation and connect the electrodes to the ground.

Eden Geothermal Ltd (EGL) initiated the contact with local landowners of the prospective locations. As site characteristics, we required at a minimum:

- Open area for the centre of the installation, not in close proximity to trees (<20m away).

- Permission to dig holes (around 50 cm in diameter, up to 1.5 m deep) for the three magnetic induction coil and five electrode (electric field) sensors.
- Vehicle access to within 100 m of the site. This may be off-road, but if so then it would preferably be less than 1 km from a metalled road.
- No livestock (sheep/cows/horses) to be present in the field at the time
- Low electromagnetic environment (e.g. 10 km from a train line, >300 m main road, >1500 m transformers and >500m buildings) where possible.
- Secure access to the land and away from public rights of way to avoid physical disturbance
- Low physical gradient and well drained soil.
- More than 1 m soil depth so that the soil can be used as insulation and connect the electrodes to the ground.

Figure 5 shows a schematic of the typical MT site layout.

EGL scouted a large portion of potential locations prior to the field campaign, providing BGS with a spreadsheet of relevant information. They also provided further support during the campaign. BGS staff followed this up during the installation period and adjusted the site locations where necessary when presented with unsuitable conditions (e.g., electric fences) that would have negatively impacted data quality, or to accommodate landowner requests (essential for the safety of equipment and crew). To the west of the Eden Geothermal site, large parts of the land are owned by the Imerys Group. As they encompass active mines, some of these areas contain mineral production and processing sites and were therefore not readily accessible. The final site locations therefore differ from the initial proposed locations.

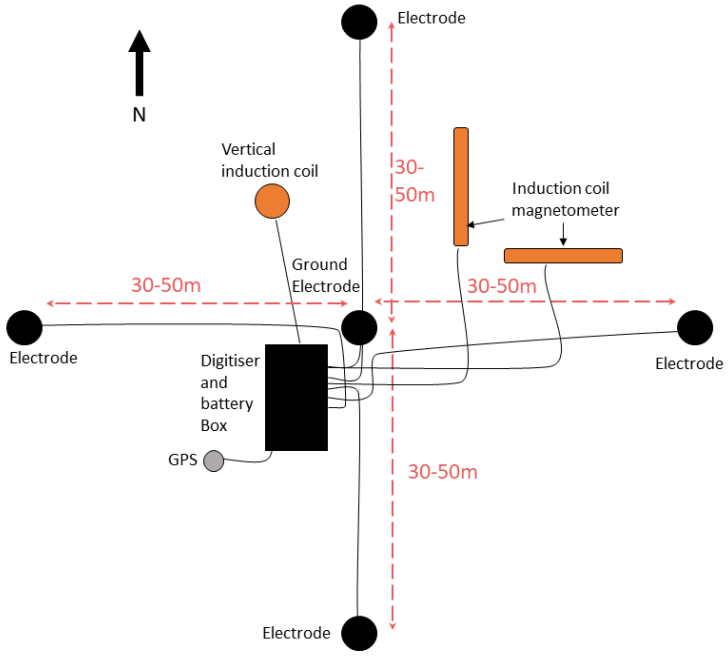

Figure 5: Setup schematics of broadband MT site. All sensors (electrodes and magnetometers) are buried to stabilise them from motion induced by wind and protect from inclement weather. BGS © UKRI. All Rights Reserved.

Five Phoenix MTU-5C MT systems were loaned from Dublin Institute of Advanced Studies (DIAS), Ireland. These are the latest version available, manufactured and delivered to DIAS in 2022 as part of a renewal of their instrument pool. Colin Hogg, a staff member from DIAS met the field crew in Cornwall at the beginning of the survey, ensured that the instruments were

running correctly and provided training on deployment, field operation and bespoke software. The systems each consist of three induction coil magnetometers measuring the magnetic field in the two horizontal and one vertical component, and four non-polarisable electrodes along two dipoles (north-south and east-west orientated, see Fig. 5). Dipole lengths are required to be > 50 m, and are at most sites around 80 m (see Table 1 in Appendix I). A fifth electrode is used to ground the system and protect against lightning. A sophisticated pre-amplifier and digitiser is part of the recording system. The electronics are placed in a weatherproof case in the centre of the installation. GPS synchronization ensures that all recordings are correctly time-stamped, and simultaneous installations could be used for remote referencing.

Each measurement period was one to two days long depending on logistics and weather, ensuring that at least one overnight period of data collection was included. At nighttime, natural signal strength is often higher while man-made noise can be lower. A site in Bodmin Moor was previously used for long-period MT data recording and deemed suitable as the remote reference location because of the relatively rural setting and lower levels of local noise influences observed [*Huebert*, 2022]. A full broadband MT system was installed there.

In total, during 11 days of field work, 100 GB of raw data were collected (Fig. 6). Data sampling was 150 Hz for continuous recording and 24 kHz for a shorter period of burst recording. All instruments were tested and calibrated at the beginning and end of the campaign. No instrument failure was noted.

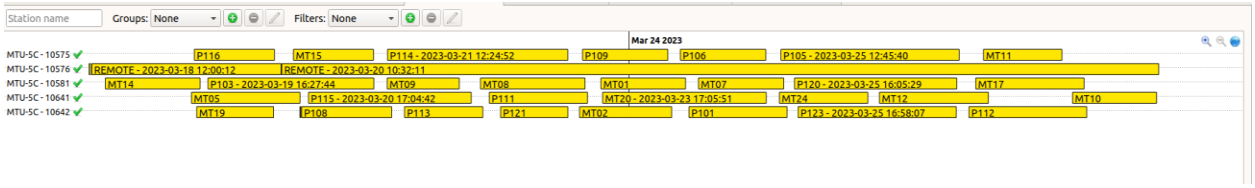

Figure 6: Deployment schedule of the five Phoenix broadband system in use during the field campaign. Simultaneous recordings can be used for remote reference processing to increase data quality significantly. Contains BGS © Data UKRI 2023. All Rights Reserved.

2.3 DATA PROCESSING TO DERIVE THE MT IMPEDANCE TENSOR

During the field campaign, data quality and recording duration times were checked before the instruments were removed from site. Copies of the data from the instruments' SD cards were made at the end of each installation. In the evenings, all sites collected that day were processed using the manufacturer's propriety software *EMPower*.

At the end of the campaign, when the data from the remote site in Bodmin moor was available, all data were reprocessed using the remote referencing technique [*Gamble et al.*, 1979]. Under the assumption that the remote site does not suffer from the same noise sources as the local site, this technique can improve the quality of the derived transfer functions through spectral analysis. Data quality can be significantly improved, especially in the so-called 'dead band' – the frequency band around 1Hz where the natural signal is quite weak. Figure 7 shows example of impedance functions derived from three sites with good quality data. Each curve is smoothly varying with small error bars indicating low noise.

Appendix 1 contains plots of the processed impedance functions from all 30 sites.

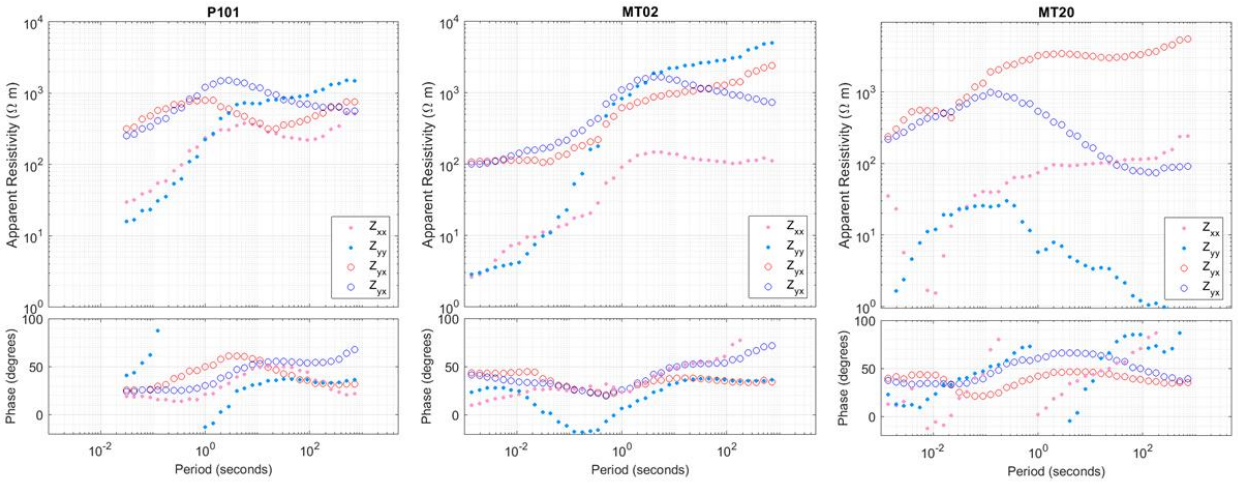

Figure 7: Apparent resistivity and phase curves for three sites, P101, MT02 and MT20. For locations see Fig. 4. Contains BGS © Data UKRI 2023. All Rights Reserved.

2.3.1 Tipper data

The vertical component of the magnetic field was measured at all sites. This allows for the calculation of the so-called tipper which is the transfer function between the horizontal and the vertical component of the magnetic field. This transfer function can also be computed at each measurement site using the same techniques as the MT impedance tensor and contains independently derived information about the resistivity structure of the subsurface. However, the quality of the raw data of the vertical magnetic component is often much lower. This is partly due to the difficulty of protecting the vertical induction coil from rain and wind when not enough topsoil is present at the site as well as the signal itself often being much smaller than the variations in the horizontal components. With the limited time available in this project, the tipper functions were computed but not used for further analysis.

2.4 DATA QUALITY

Serendipitously during the field campaign a moderate (G4) geomagnetic storm during the night 23- 24 March (maximum: Kp 8^0) was captured. The geomagnetic storm is seen as pulsations in the raw data in Figure 8. The increased signal strength resulted in good data quality at the sites recorded during that time (MT01, MT02, MT20 and P109).

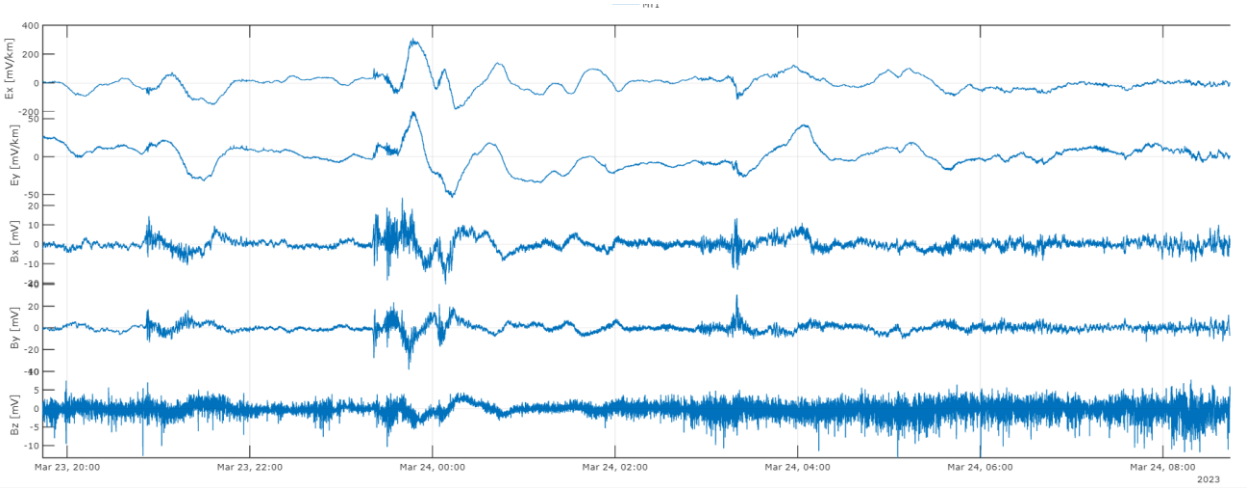

Figure 8: Raw timeseries data recorded at site MT01 during the 23/24 March G4 storm. Increased geomagnetic activity is observed as strong longer wavelength pulsations. Contains BGS © Data UKRI 2023. All Rights Reserved.A detailed analysis of site location and data

quality can be found in Appendix 1. In general, the site location further away from the towns and houses had the best data quality, with sites MT01, MT02 and MT20 having the smoothest impedances and smallest data errors.

When cultural noise is very strong, it completely dominates the signal in the electric channels. In those situations, even the remote reference technique cannot help and the data have to be disregarded. For our data as set, we had to exclude the data from following site: MT08, MT10, MT17, P103, P106, P111, P112, P121.

3 Three-dimensional inverse modelling

The derived MT impedances can now be used to find a plausible electrical resistivity model of the area at depth. In the last two decades advances in computer architecture and computational algorithms have made it feasible to analyse MT data with 3D inversion algorithms. These are mathematical tools to create gridded resistivity models through non-linear inversion techniques with the goal of explaining the data with the lowest reasonable misfit. Furthermore, prior information like topography, bathymetry and smoothness constraints can be inbuilt into the process. The depth extent and resolution of the derived models depends on the frequency bandwidth of the data and the lateral site spacing. Resolution also depends on the conductivity in the model itself.

However, the amount of useful data (21 sites) in the St Austell area does not allow for a high-resolution inverse model. Recent examples of MT studies using 3D inversion typically require 50+ sites (but often many more [*Tschirhart et al.*, 2022]) for sufficiently dense spatial sampling. Nevertheless, 3D inversion of the collected data was performed to investigate if a model can be found that both is supported by the data and contains recognisable geological features, such as the assumed high resistivity of the St Austell granite.

3.1 3D INVERSION PROCEDURE

For the 3D inversion we used the ModEM software, a powerful data space inversion code [*Kelbert et al.*, 2014] that can run in parallel on High Performance Computing (HPC) architecture. It uses a finite difference scheme on a staggered grid to solve Maxwell's equations using a non-linear conjugate gradient solver. It requires the modelling domain to be discretised with a regular grid. Both topography and bathymetry can be included by fixing the resistivity values of certain cells to either very high for air cells and very low (typically 0.3 Ωm) for seawater cells.

For the inversion computations of the St Austell data, we used the BGS Linux HPC cluster. The memory and run time required per inversion depend heavily on the amount of data and the number of cells in the model. Numerous runs are necessary to find the optimal inversion parameter set and a suitably resolved grid. The guiding parameter is the achievable data fit, here expressed as a normalized root-mean-square (RMS), taking the data error into account.

For a perfect fit, the RMS would be 1, though for noisy data or low spatial resolution it can be higher and only a local minimum of the optimisation function can be found. The extent of the grid is a trade-off between the overall size of the modelling domain, the distance between sites as well as vertical discretization and the computational costs. We chose a model discretisation with 274 m horizontal cell size (to allow for free cells between station locations) in the central part of the model and added growing padding cells. For the vertical cell size, we started with 10 m, increasing with a factor of 1.2 in each subsequent layer. The number of cells is 88x88x48 and the model dimensions are 218 km x 218 km x 1097 km. Each inversion setup took 24-30 hours before the convergence criteria was reached or a local minimum was found. Figure 9 shows the configuration of the cells for the surface layer at the initialisation of the model.

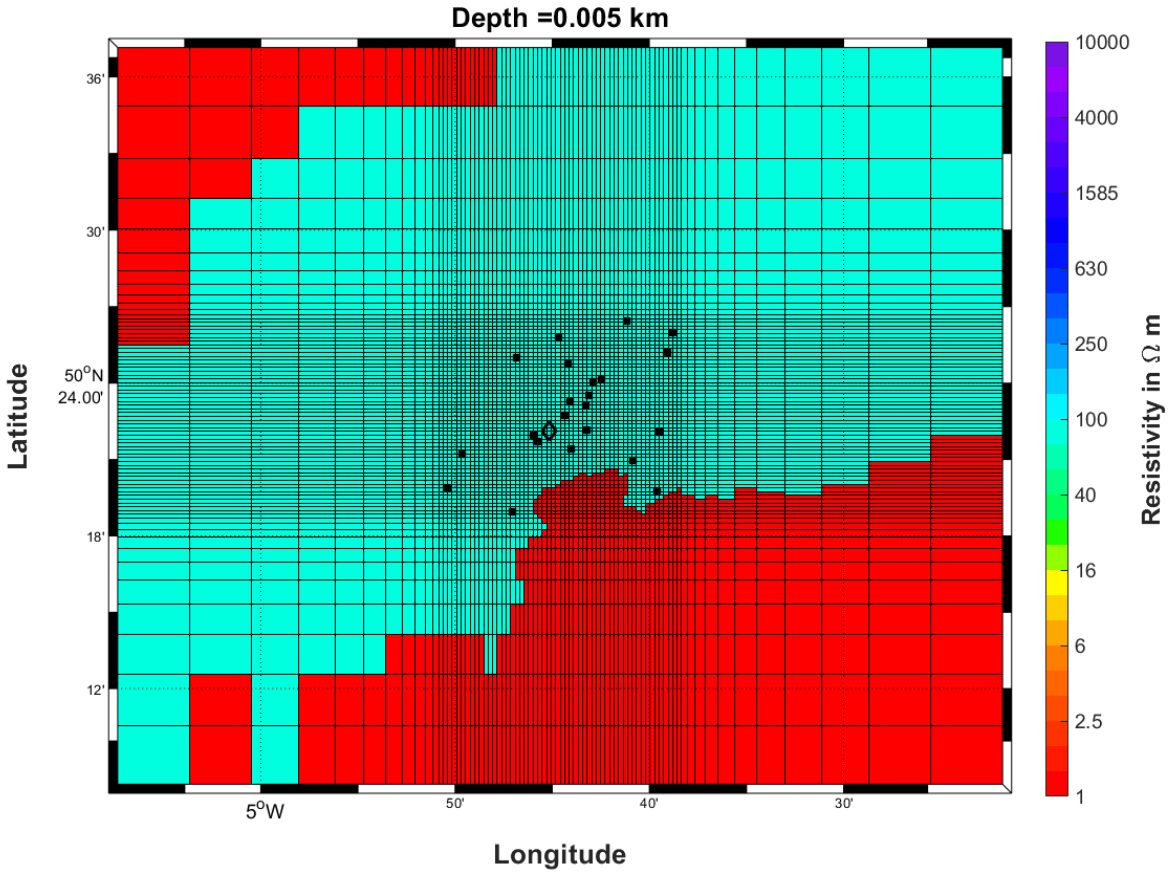

Figure 9: Surface of starting model with sea water in upper layer. The squares indicate the position of the MT sites in the grid, the diamond shape the location of the Eden drill site. Red cells have seawater resistivity of 0.3 Ωm, the green cells have a background resistivity of 100 Ωm. Additional padding cells not shown. The land part of the model is assumed to have flat topography. Contains BGS © Data UKRI 2023. All Rights Reserved.

Following best practise [*Robertson et al.*, 2020], the inversion parameter tested were: the data error floor (varied between 5%, 7% and 10% of the off-diagonal elements, 5% was chosen for the presented model), the background resistivity of the starting model at depth (10, 100 and 1000 Ωm; 100 Ωm in the presented model) and the covariance of the model (to regulate the trade-off between a smooth model and data fit). The parallelisation is across the number of frequencies of the data (we chose 20 frequencies between 1000 Hz and 0.00195 Hz). The impedance curves were cleaned from outliers and smoothed as preparation for the inversion.

Firstly, the off-diagonal impedance elements Zxy and Zyx were inverted using a half-space starting model including bathymetry. Once this converged (starting from an RMS of 12), the final iteration of this run was used for a new inversion run using the full impedance elements. Finally, the model covariance was applied. The RMS fit for the off-diagonal inversion run was 1.5, for the full impedance 2.0, indicating that the diagonal impedance tensor elements could not be fitted as well with the error floors chosen. This is especially the case for sites where the diagonal elements are much smaller than the off-diagonals (e.g., MT20).

For the final model, we inverted all impedance tensor elements simultaneously, achieving a RMS fit of 2.0 after 96 iterations. For the final data fit see plots in Appendix 1, Section 3.

Figure 10 displays the RMS for each site. Most sites have good data fit below 2 with a few outliers that should be investigated further or excluded in future inversion when more data is available.

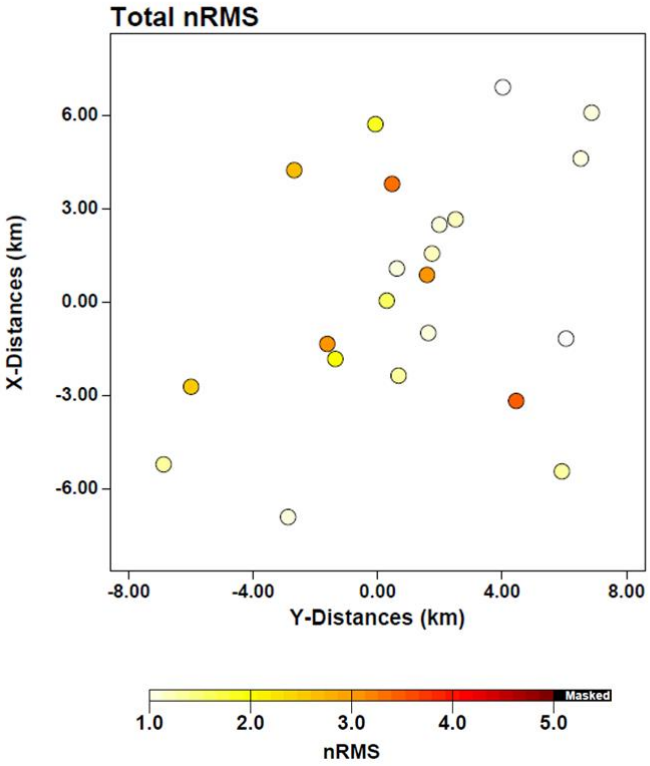

Figure 10: Normalised RMS fit per site in map view for the response impedance elements of the presented model. Contains BGS © Data UKRI 2023. All Rights Reserved.

4 A low-resolution electrical resistivity model of the St Austell area

The final three-dimensional model is the result of our initial study and further refinement is possible with more time and data. Nevertheless, it shows that modern MT measurements can produce valid models in this semi-urban setting.

Our final model is presented from different viewpoints in Figures 11, 12 and 13 and shows large contrasts of electrical resistivity between 10 and 3000 Ωm especially at shallow depths. Figure 11 depicts depth slices through the model in map view. In the shallower layers, the model shows very patchy lateral resistivity variations which are due to the coarse spatial sampling. This occurs where the spacing between the sites is larger than the skin depth or induction length of the higher frequencies. From 500 m below mean sea level the model regularisation allows for a smoother image to form and starts to depict high resistivities beneath most of the sites at the centre of the array. The southern region of the model area is dominated by lower resistivities, stemming from the offshore sediments in St Austell Bay. The resistive features, presumably associated with the St Austell granite (see Fig. 12), are very dominant in the model down to 5 km.

In general, the coarse spatial data sampling does not allow for an exact lateral characterization of the St Austell granite and the interspersing conductors. This could only be achieved by collecting more data on a denser spatial grid. Nevertheless, there are interesting lateral changes in resistivity within the St Austell granite that could be studied further. Of most interest is a more conductive zone to the SE of the EGL drill site (visible in the depth slices in Figure 11). The northwest end of the surface trace of the GXC Fault could not be constrained because of a paucity of data here (due to land access issues). Below 6 km the model does not diverge from the background resistivity of 100 Ωm, indicating that data resolution is too low to impart any further information.

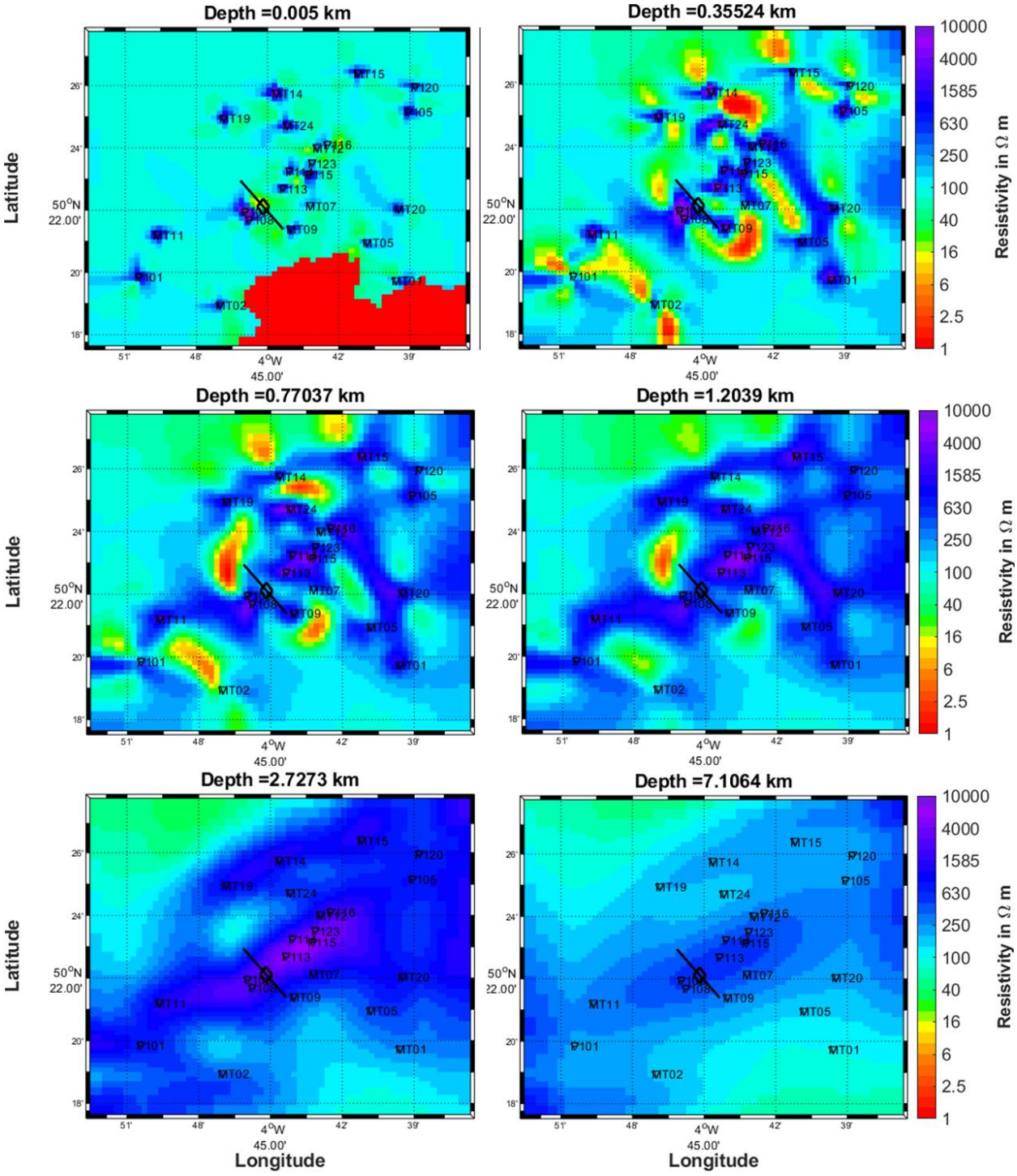

Figure 11: Depth slices through the presented resistivity model at 5 m, 350 m, 770 m, 1200 m, 2727 m and 7106 m below mean sea level. Padding cells are not shown. Site locations are indicated with triangles and site names. The inferred surface occurrence of the GXC Fault is indicated with the black line, the black diamond shows the position of the EGL drill site.

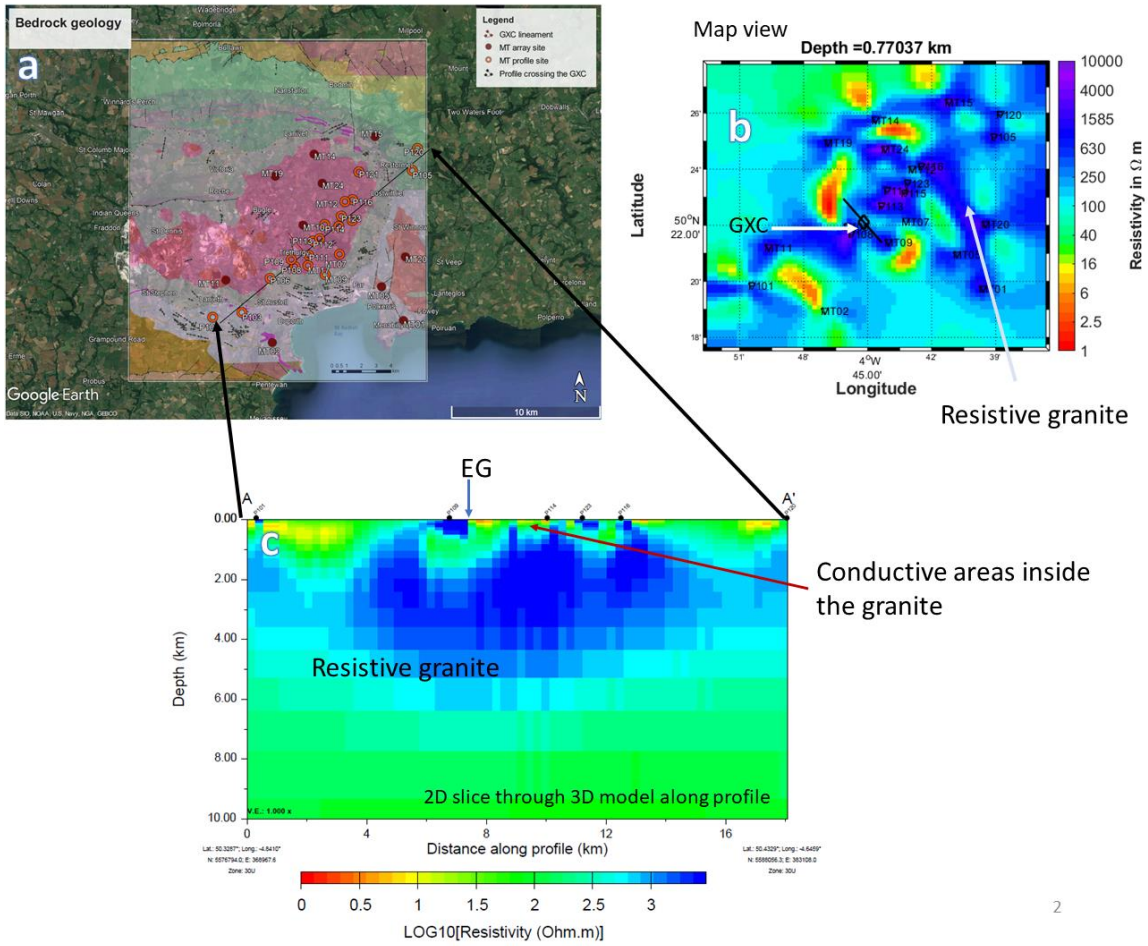

Figure 12: a) Geologic map with MT site locations, b) model depth slice at 770 m below mean sea level and c) profile section. Contains BGS © Data UKRI 2023. All Rights Reserved.

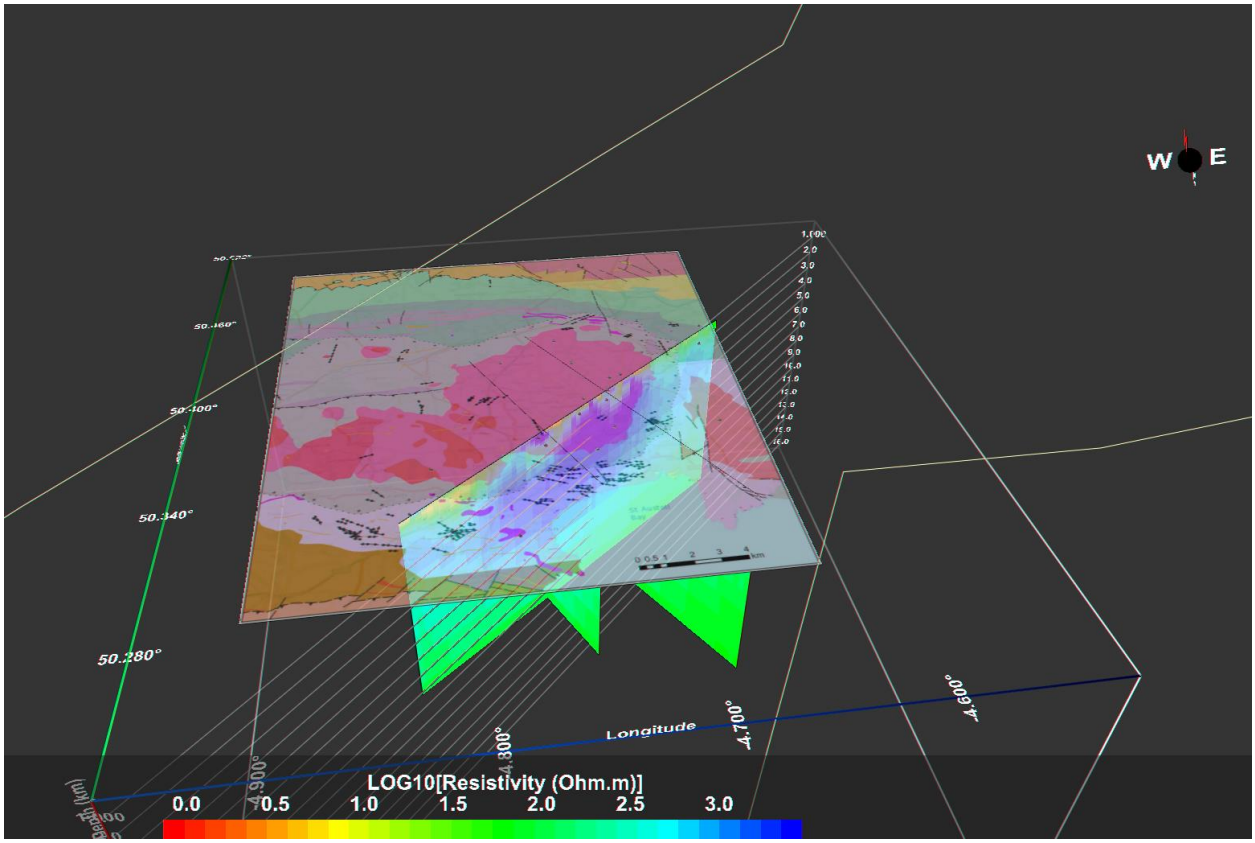

Figure 13: 3D view of vertical model slices down to 7 km, crossing the EG drill site with view from S. The geologic map from Figure 2 is shown for orientation. Contains BGS © Data UKRI 2023. All Rights Reserved.

5 Conclusions and Recommendations

In this pilot study we investigated the feasibility of collecting magnetotelluric data to study geologic structures at depth for geothermal exploration. We collected 30 broadband MT sites in the St Austell area in Cornwall. Data quality was challenging due to the semi-urban environment including many sites with artificial electromagnetic noise sources like electric fences and other infrastructure. The area in close vicinity to the Eden Project compound suffered especially from very low signal-to-noise ratios. Using a remote site in Bodmin Moor we were able to compute MT impedances and used the medium to good quality MT data at 21 sites to derive a low-resolution 3D inversion model of the electrical resistivity in the area.

The MT data can be reasonably well fitted with a model of electrical resistivity by including fixed cells for the sea water in the offshore parts of the model around the Cornish peninsula. The derived model depicts high resistivity in the location of the St Austell granitic intrusion, mapping it to a depth of 5-6 km. The St Austell Bay area shows lower resistivities corresponding to sedimentary rocks. There are some zones of lower resistivity in the granites as well, but the low resolution related to the coarse spatial site sampling in this pilot study means it is not possible to definitely associate them with fracture zones. However, with more data of sufficient quality and more detailed modelling and sensitivity studies it would be possible to characterize these interesting NW-SE striking conductive features in more detail.

We would recommend collecting more broadband MT data, especially in the NW vicinity of the Eden Geothermal Ltd drill site, where land access was not available during the field campaign. For full and comprehensive 3D inverse modelling, data from at least 50 sites in the area would be necessary. To image the zone around the borehole at depths of >2 km in higher resolution, we suggest controlled-source EM methods, using an electric dipole of sufficient strength for controlled source MT. This would allow to overcome the local noise problem in the vicinity of build-up areas.

Overall, the objectives of the study were met and the utility of MT measurements in a semi-urban environment has been assessed.

Appendix 1

1. SURVEY DETAILS

This section contains detailed descriptions on the locations of all MT sites, the duration of data recording at each site, the MTU identifiers, the dipole lengths and the induction coil numbers that are necessary for system response correction during time series processing.

Table 1: Survey details. Contains BGS © Data UKRI 2023. All Rights Reserved.

Station Name	Start Time	Instrument ID	H1 serial #	H2 serial #	H3 serial #	E1 dipole [m]	E2 dipole [m]	Duration	Altitude [m]	Latitude [Deg]	Longitude [Deg]
MT01	Thu Mar 23 2023 16:41:51	10581	57447	57432	57426	89.0	87.1	20h 41m 48s	119	50.329247	-4.65982
MT02	Thu Mar 23 2023 11:26:36	10642	57422	57425	57442	88.5	95.0	22h 33m 5s	138	50.316058	-4.783727
MT05	Sun Mar 19 2023 12:24:25	10641	57428	57440	57446	100	100	1d 2h 35m 21s	85	50.349621	-4.680486
MT07	Fri Mar 24 2023 16:34:02	10581	57447	57432	57426	85.4	85.5	20h 51m 24s	164	50.369255	-4.720254
MT08	Wed Mar 22 2023 11:12:01	10581	57447	57432	57426	87.9	83.6	1d 1h 35m 5s	205	50.389593	-4.708163
MT09	Tue Mar 21 2023 12:20:41	10581	57447	57432	57426	84.7	87.3	17h 37m 30s	159	50.356937	-4.73372
MT10	Tue Mar 28 2023 12:08:36	10641	57428	57440	57446	88.7	81.0	20h 36m 36s	185	50.386813	-4.75466
MT11	Mon Mar 27 2023 14:21:29	10575	57449	57421	57423	87.4	77.2	19h 12m 43s	247	50.353723	-4.827609
MT12	Sun Mar 26 2023 12:52:14	10641	57428	57440	57446	81.2	90.6	1d 2h 40m 54s	260	50.40056	-4.715244
MT14	Sat Mar 18 2023 15:20:33	10581	57447	57432	57426	83.0	85.8	23h 10m 48s	224	50.429604	-4.744198
MT15	Mon Mar 20 2023 13:22:54	10575	57421	57449	57423	71.5	79.3	19h 36m 11s	103	50.440286	-4.686549
MT17	Mon Mar 27 2023 12:27:14	10581	57447	57432	57426	58.7	63.3	1d 2h 31m 16s	184	50.362413	-4.750035
MT19	Sun Mar 19 2023 13:42:21	10642	57422	57425	57442	79.2	89.2	18h 49m 7s	193	50.416321	-4.780936
MT20	Thu Mar 23 2023 17:05:51	10641	57428	57440	57446	89.4	86.5	1d 16h 3m 28s	88	50.367646	-4.657939
MT24	Sat Mar 25 2023 12:22:17	10641	57428	57440	57446	90.4	93.0	21h 40m 34s	182	50.412352	-4.736627
P101	Fri Mar 24 2023 14:15:07	10642	57422	57425	57442	86.5	84.0	24h 0m 9s	152	50.331284	-4.84004
P103	Sun Mar 19 2023 16:27:44	10581	57447	57432	57426	85.4	82.6	1d 16h 36m 29s	159	50.334198	-4.812741
P105	Sat Mar 25 2023 12:45:40	10575	57421	57449	57423	70.2	76.4	1d 19h 38m 39s	180	50.419666	-4.651286
P106	Fri Mar 24 2023 12:07:17	10575	57421	57449	57423	73.2	79.8	20h 55m 9s	239	50.355559	-4.786192
P108	Mon Mar 20 2023 15:23:58	10642	57422	57425	57442	86.5	86.4	22h 1m 34s	206	50.361731	-4.762346
P109	Thu Mar 23 2023 12:10:38	10575	57421	57449	57423	53.7	79.0	20h 53m 6s	227	50.366094	-4.765967
P111	Wed Mar 22 2023 13:20:20	10641	57428	57440	57446	51.8	44.5	24h 2m 35s	198	50.368617	-4.749308
P112	Mon Mar 27 2023 10:48:06	10642	57422	57425	57442	86.1	86.8	1d 4h 49m 8s	180	50.37726	-4.745439
P113	Tue Mar 21 2023 16:36:09	10642	57422	57425	57442	83.8	90.1	19h 9m 25s	172	50.378618	-4.739052
P114	Tue Mar 21 2023 12:24:52	10575	57421	57449	57423	71.2	78.2	1d 20h 8m 43s	154	50.387897	-4.734478
P115	Mon Mar 20 2023 17:04:42	10641	57428	57440	57446	88.3	87.2	1d 15h 50m 31s	212	50.386059	-4.720824
P116	Sun Mar 19 2023 13:07:35	10575	57421	57449	57423	67.1	77.1	19h 36m 43s	220	50.402115	-4.707907
P120	Sat Mar 25 2023 16:05:29	10581	57447	57432	57426	87.4	90.6	1d 15h 42m 50s	188	50.432935	-4.646376
P121	Wed Mar 22 2023 16:06:40	10642	57422	57425	57442	82.4	91.9	16h 28m 15s	192	50.418843	-4.701879
P123	Sat Mar 25 2023 16:58:07	10642	57422	57425	57442	88.5	79.1	1d 14h 43m 24s	236	50.392231	-4.71857
REMOTE	Sat Mar 18 2023 12:00:12	10576	57424	57448	57439	85.0	89.0	1d 22h 21m 46s	324	50.587877	-4.622895
REMOTE	Mon Mar 20 2023 10:32:11	10576	57424	57448	57439	85.0	89.0	8d 22h 43m 48s	324	50.587877	-4.622895

5.1 SITE LOCATIONS AND MT IMPEDANCES

This section contains detailed description and satellite images of the site locations, a brief description on potential noise sources in the area and a plot for single site processed and remote reference processed MT impedances (off diagonal elements as apparent resistivity and phases).

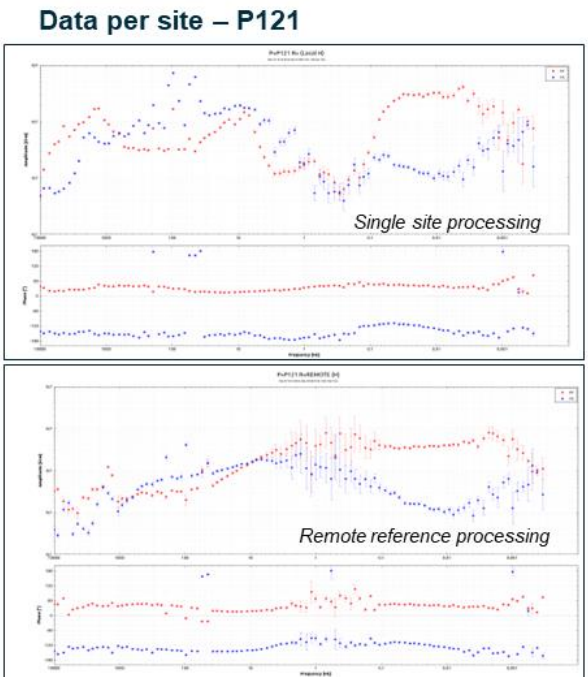

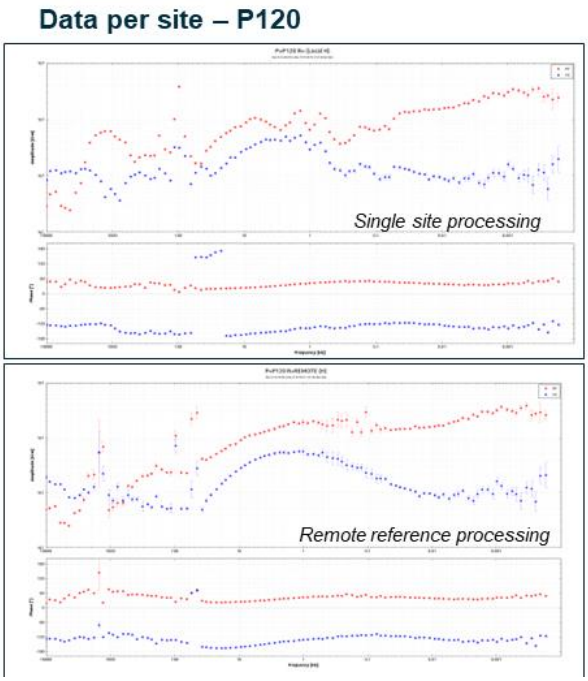

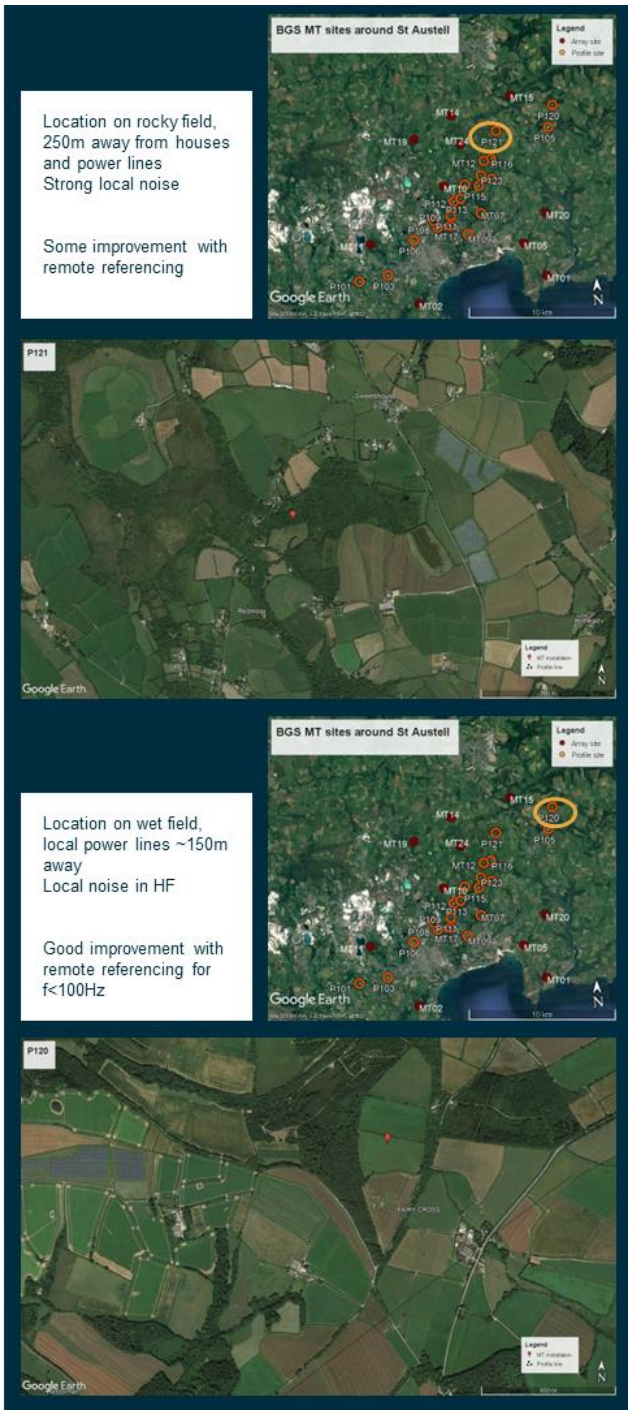

Data per site – P116

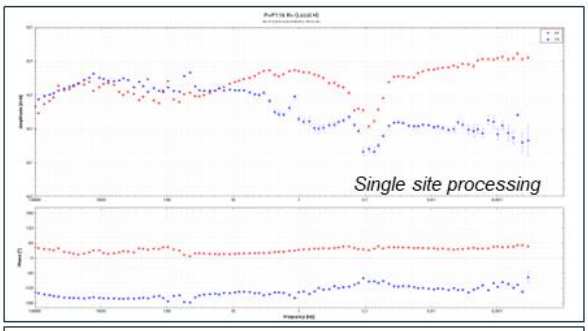

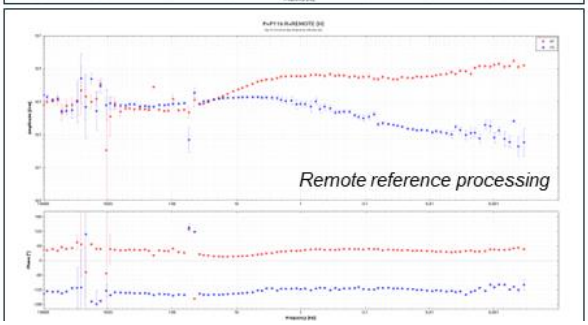

Location on pasture, 150m away from house and local power line
Some noise

Good improvement with remote referencing

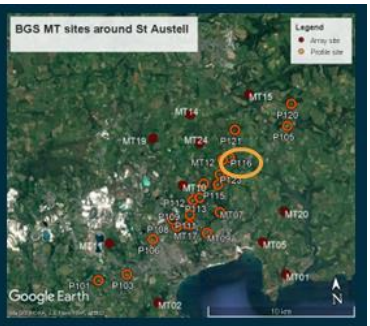

Data per site – P115

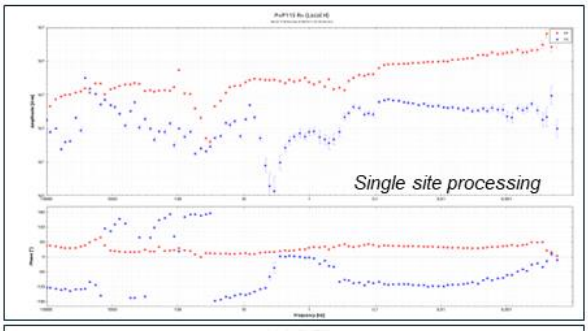

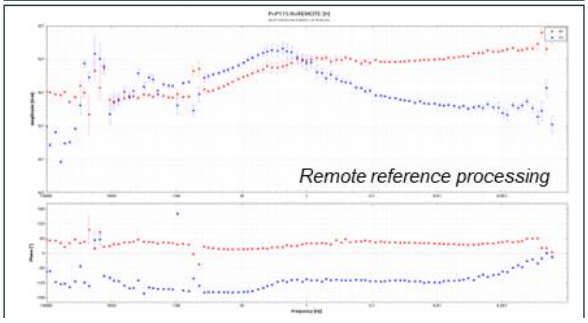

Location on pasture, 100m to next power line, electric fences nearby, 1km to railway

HF noise

Good improvement with remote referencing

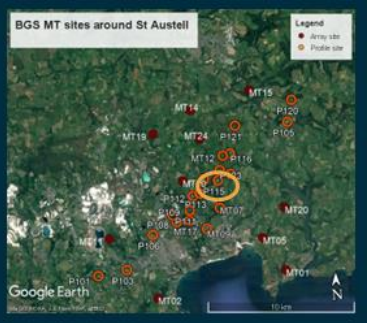

Data per site – P114

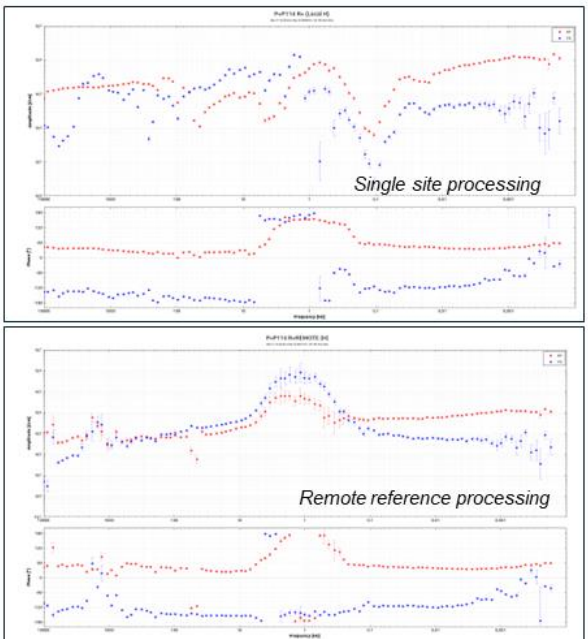

Location on pasture, ~100m away from railway tracks

Improvement with remote referencing, except in dead band where coherent noise persists

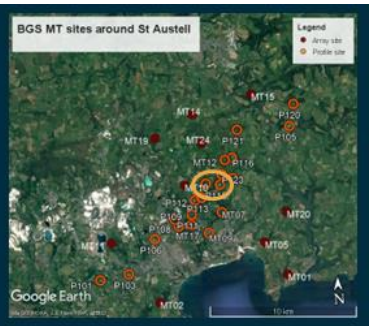

Data per site – P113

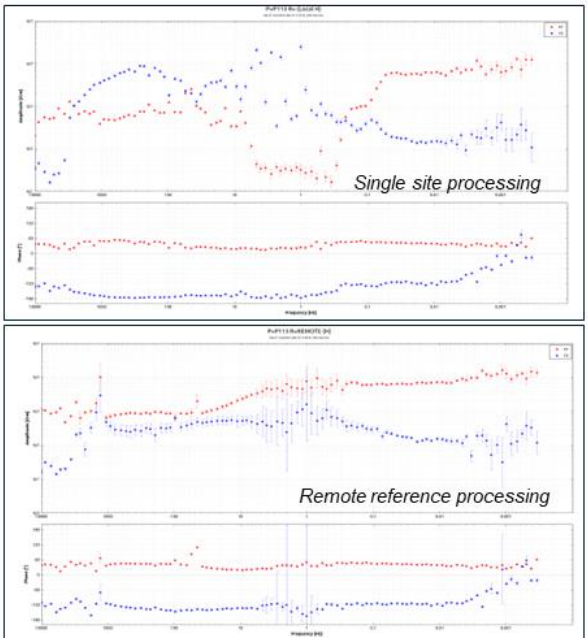

Location on pasture, close to cow shed
Very noisy data

Good improvement with remote referencing except in dead band (~1s)

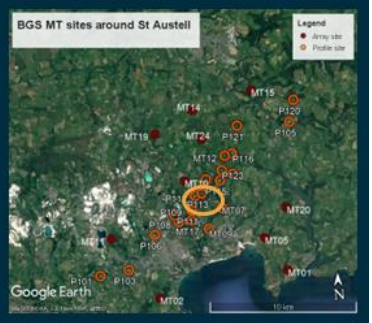

Data per site – P112

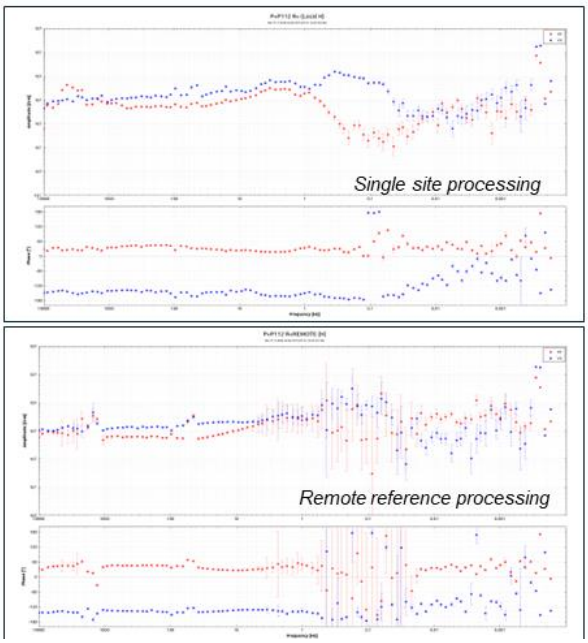

Location on field, electric power lines close by
HF data looks OK, long period data very noisy

Only small improvement with remote referencing

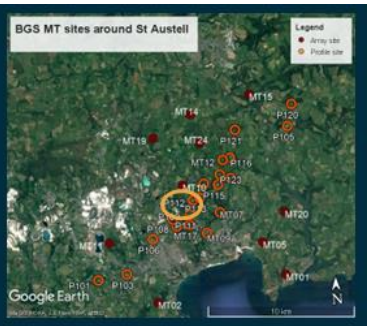

Data per site – P111

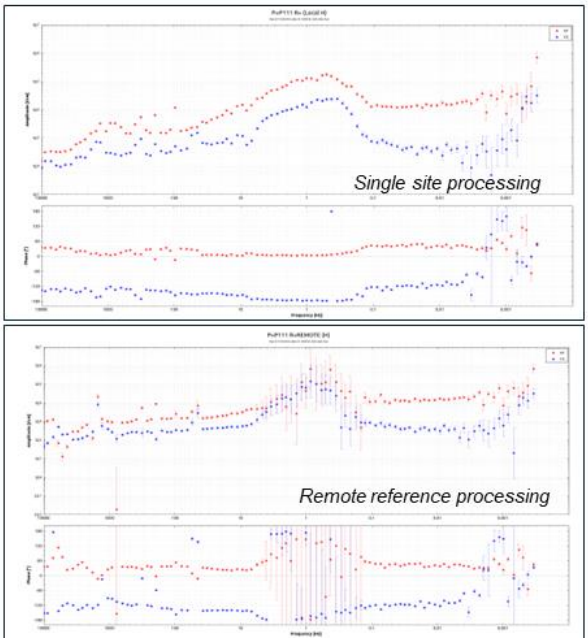

Location very close to Eden drill site, on small field close to houses
Strong coherent noise

Small improvement with remote referencing

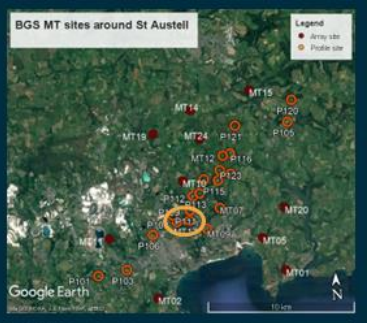

Data per site – P109

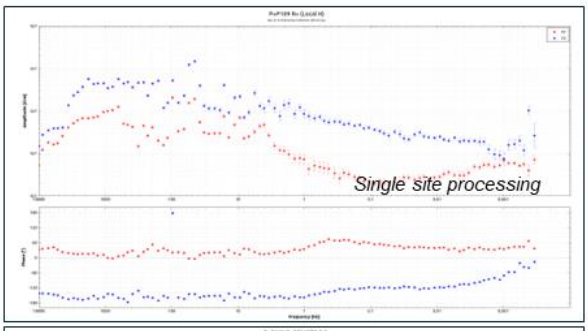

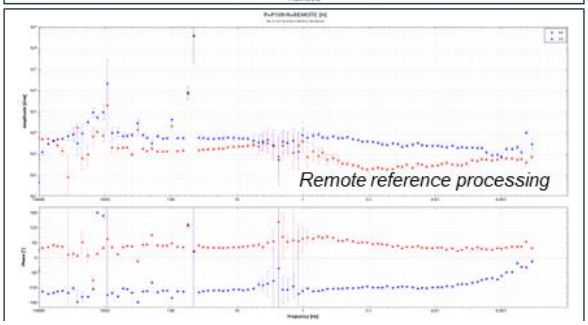

Data per site – P108

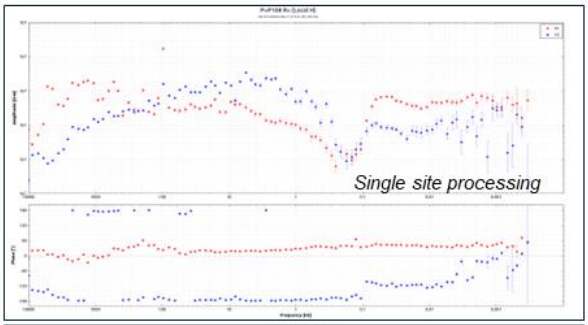

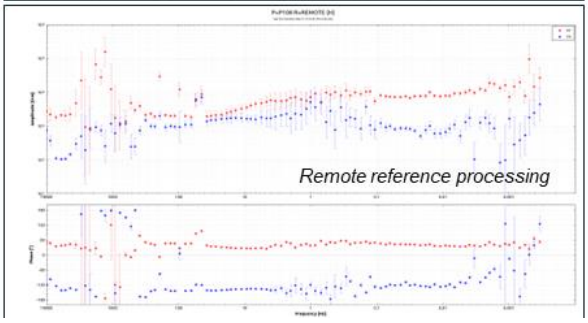

Location close to houses (<100m), electric fence for horse was switched off, close to industrial site
Noisy data

Partial Improvement with remote referencing

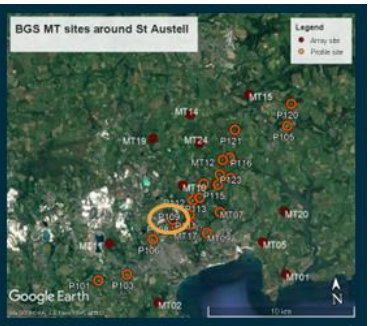

Location on pasture, very close to St Austell, powerlines ~200m away, electric fences nearby

Strong coherent noise
Some improvement with remote referencing

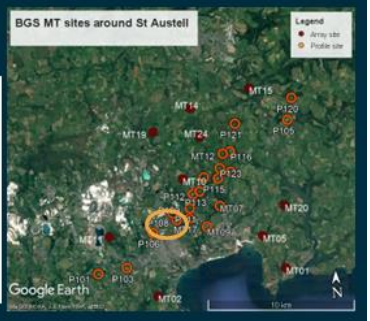

Data per site – P106

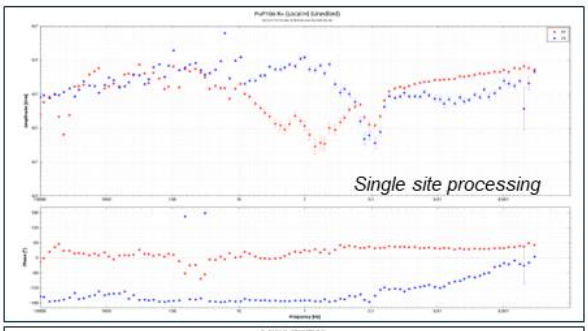

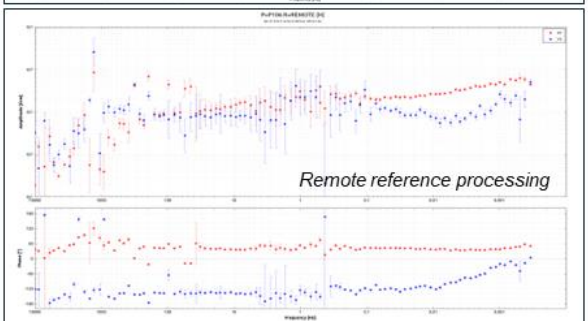

Location on pasture, very close to St Austell, a transformer and a tower, electric fences

Strong coherent noise
Very little improvement with remote referencing

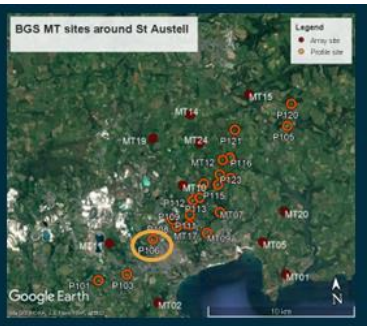

Data per site – P105

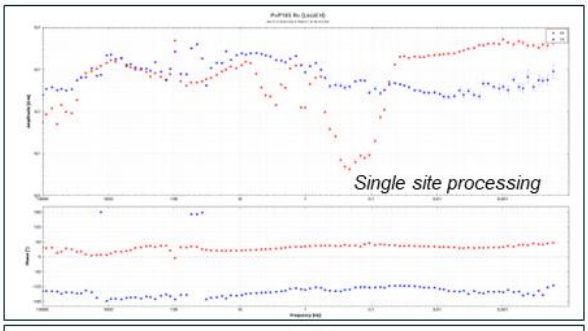

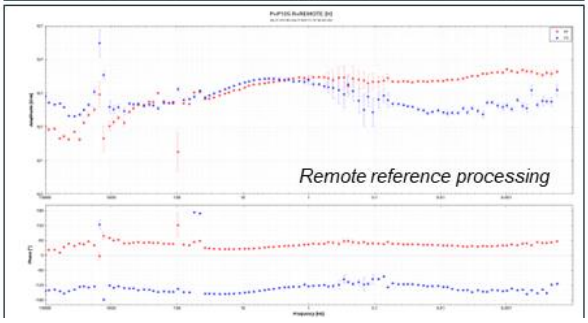

Location: power lines at the edges of the field

Noisy data

Good improvement with remote referencing

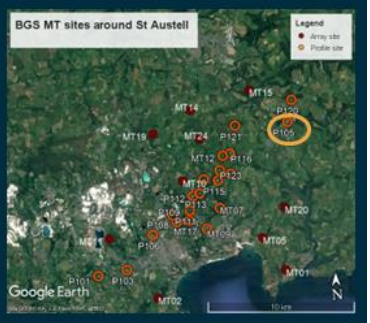

Data per site – P103

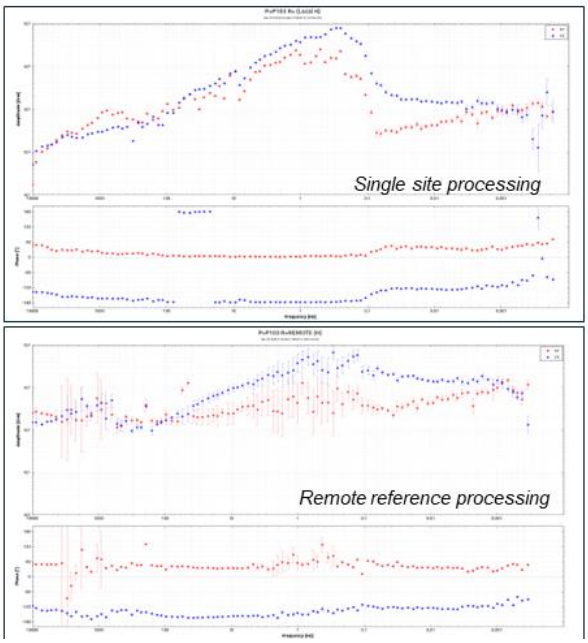

Location on a field, very close to St Austell, transformer close by

Coherent noise in the deadband (~1s), Little improvement with remote referencing

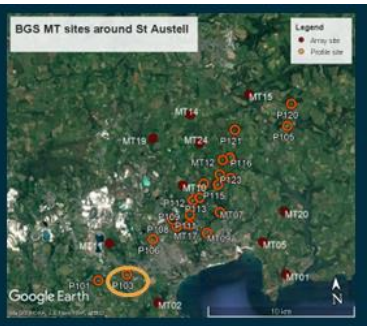

Data per site – P101

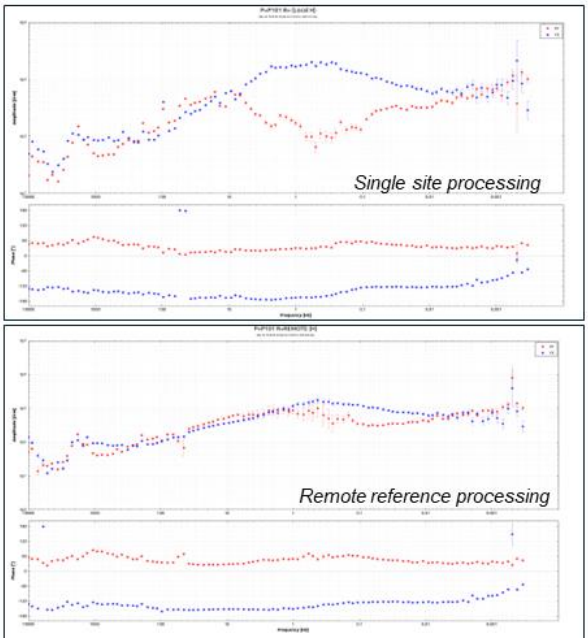

Location on a field, at least 200m away from nearest power line

Some noise in the deadband (~1s), Good improvement with remote referencing

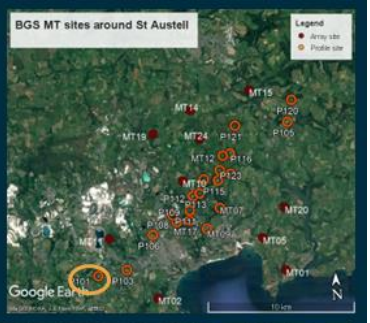

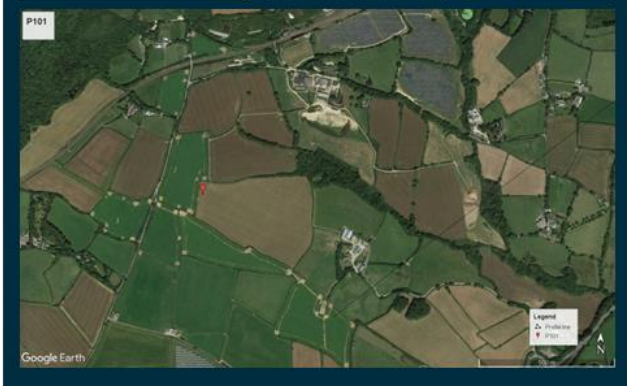

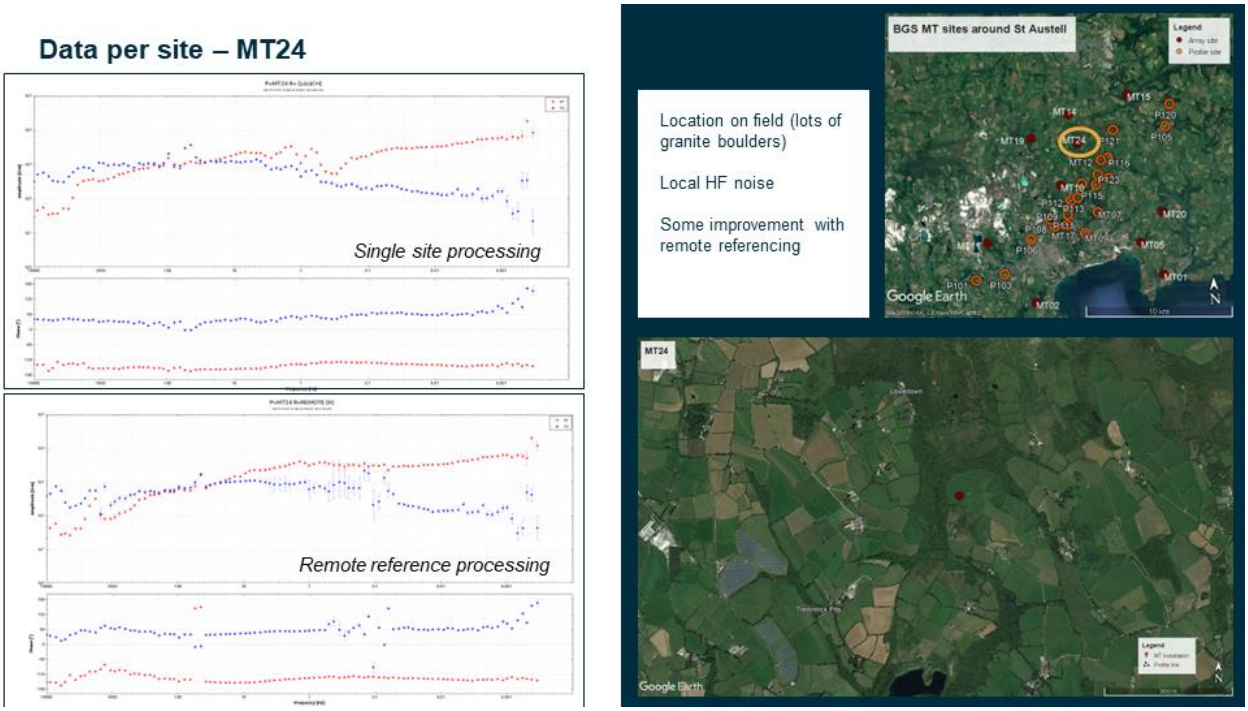

Data per site – MT20

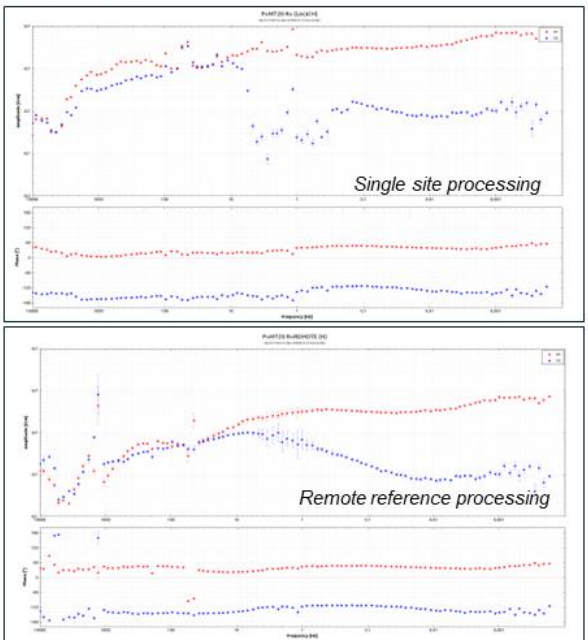

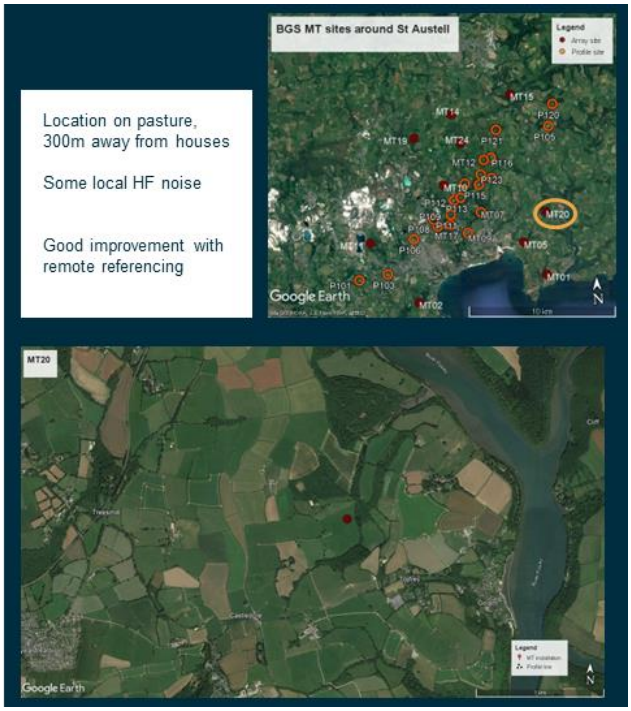

Data per site – MT19

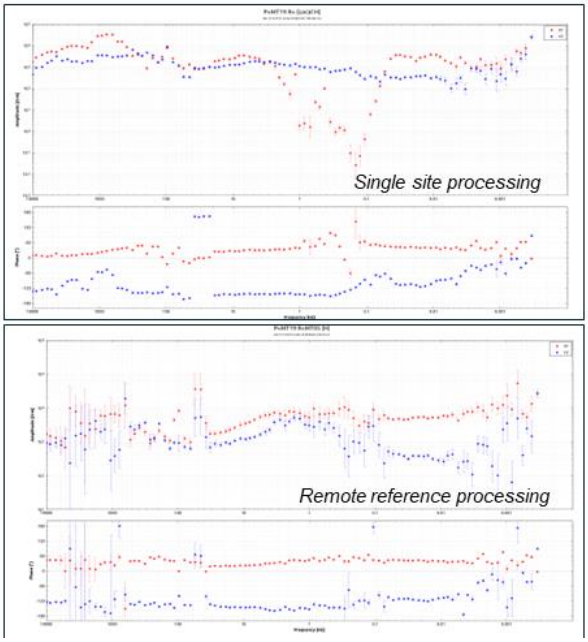

Data per site – MT17

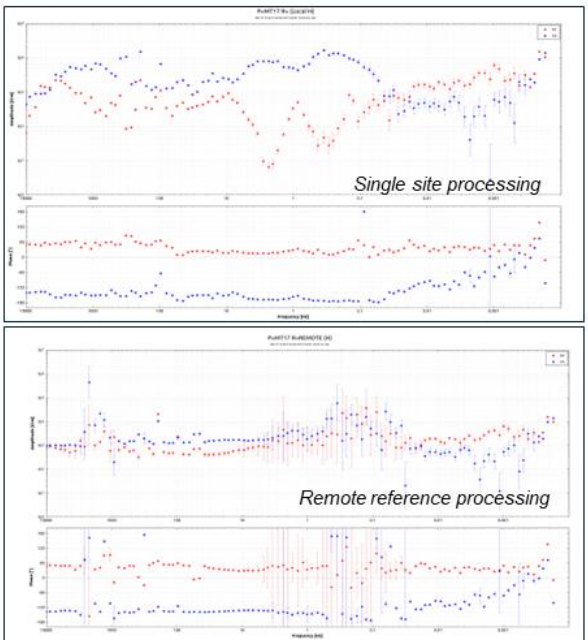

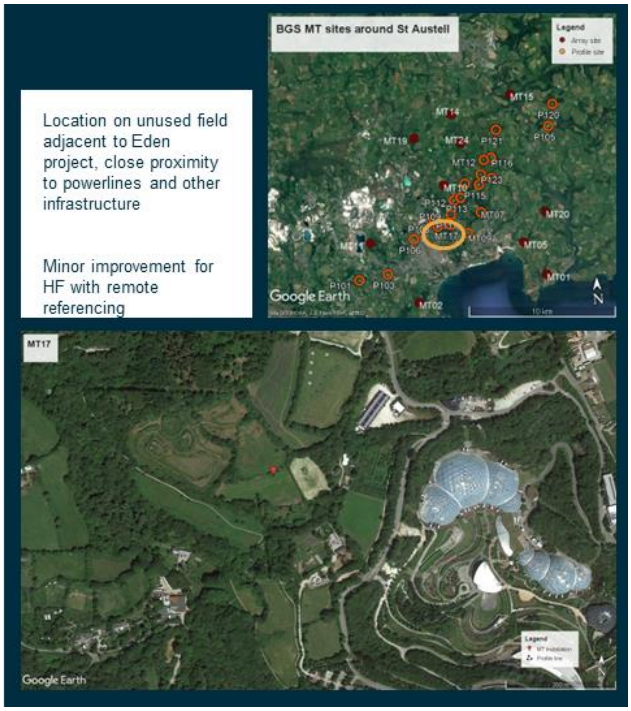

Data per site – MT15

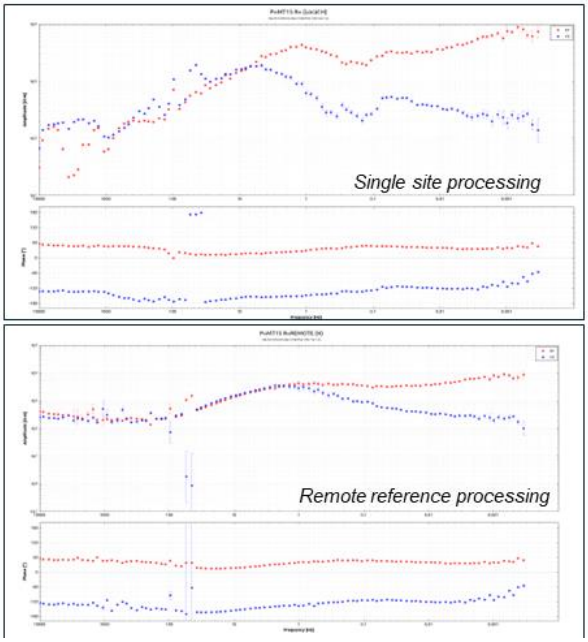

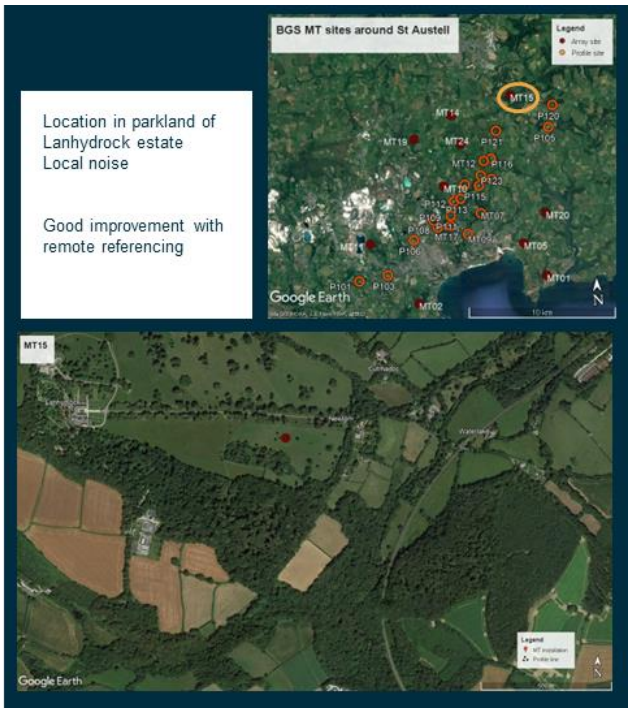

Data per site – MT14

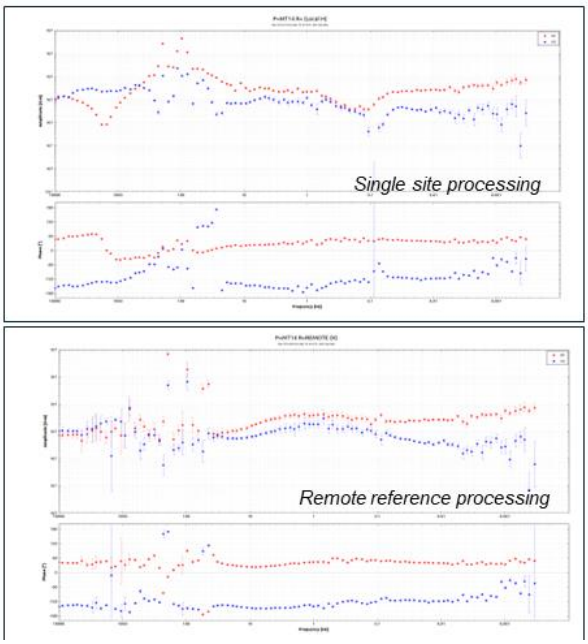

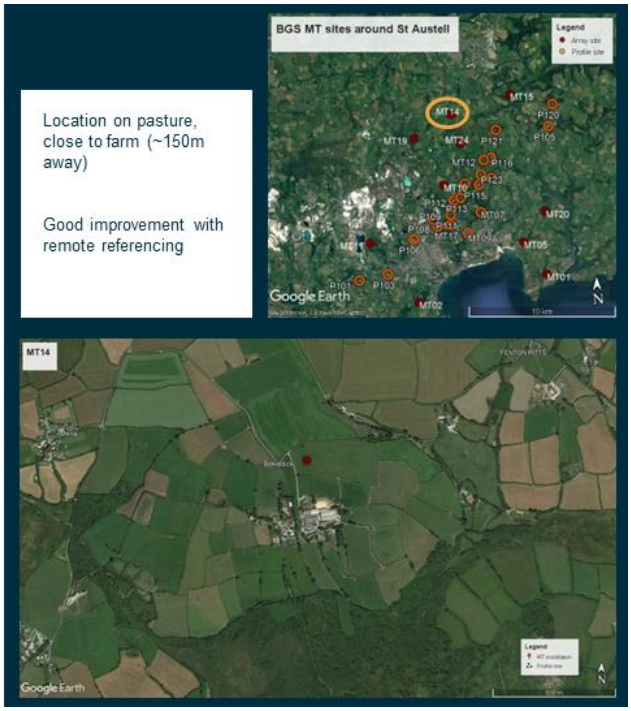

Data per site – MT12

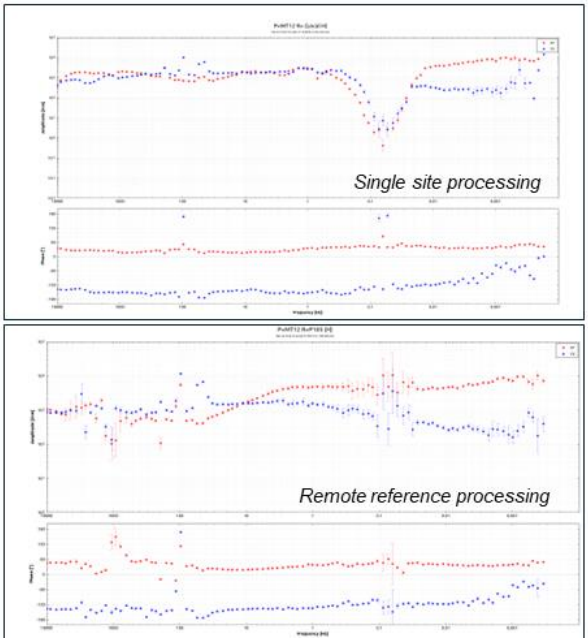

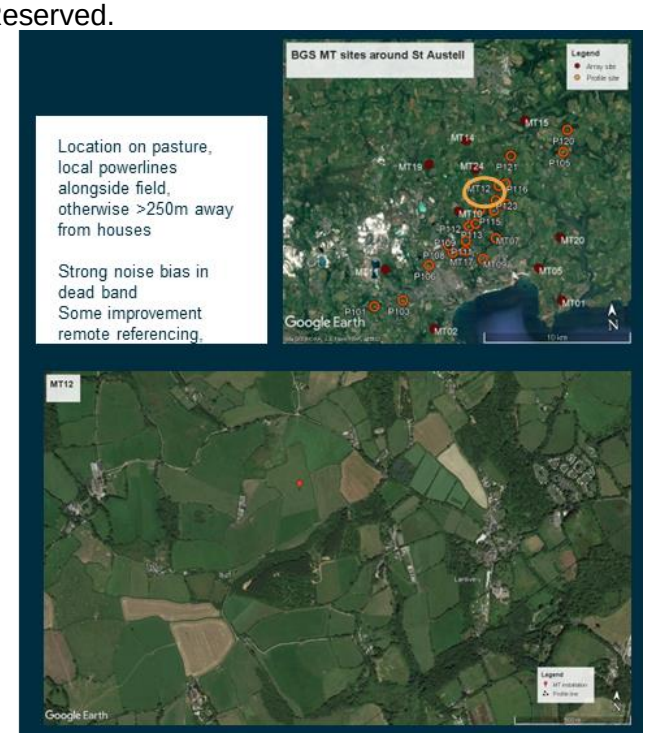

Data per site – MT11

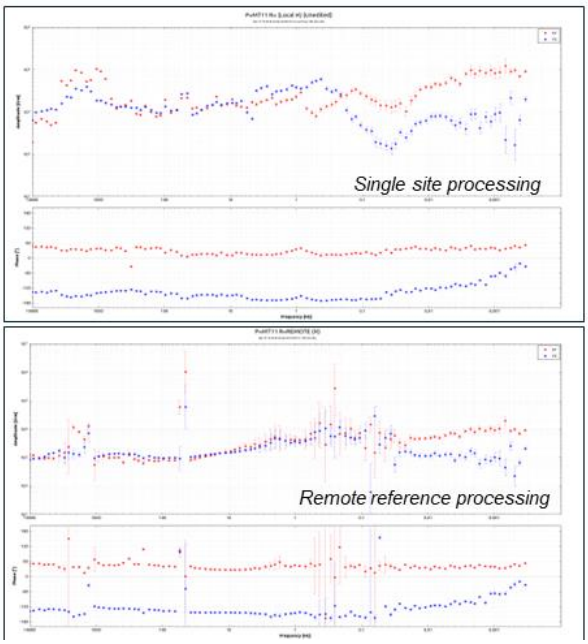

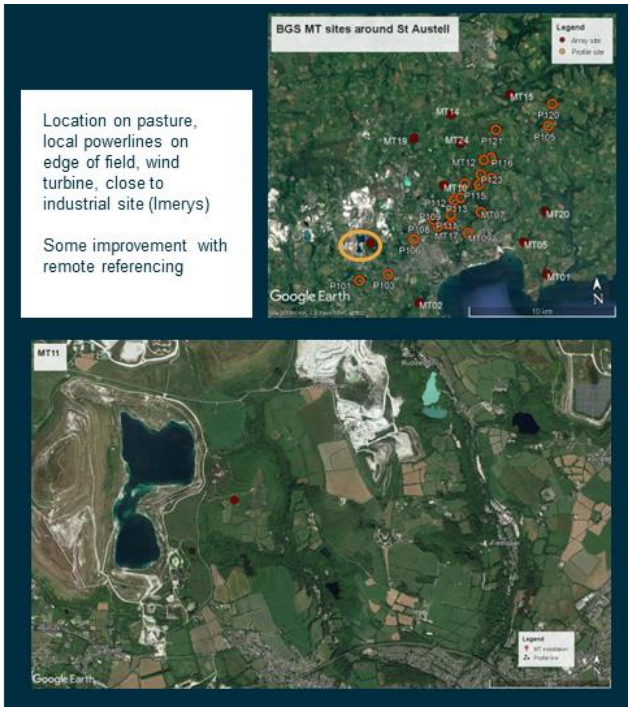

Data per site – MT10

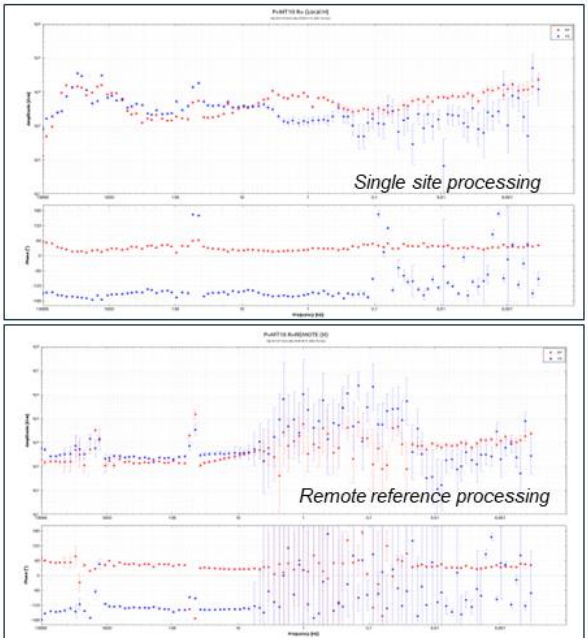

Data per site – MT09

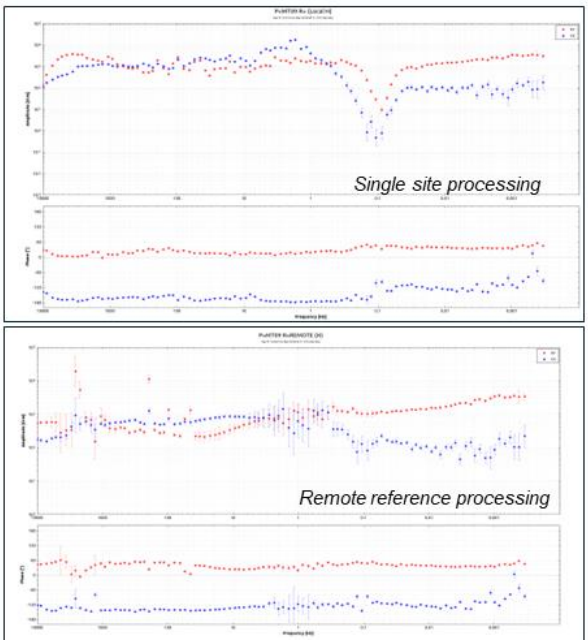

Data per site – MT08

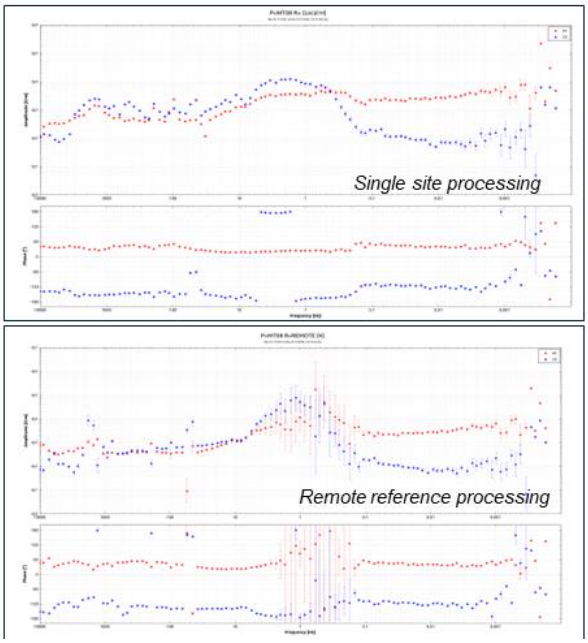

Data per site – MT07

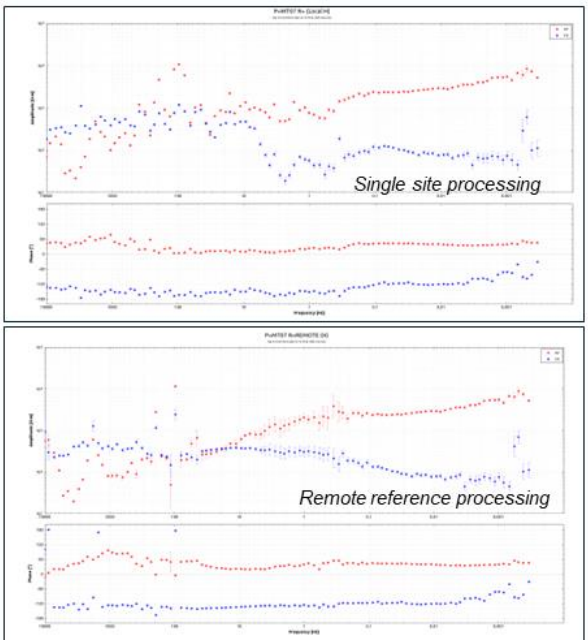

Data per site – MT05

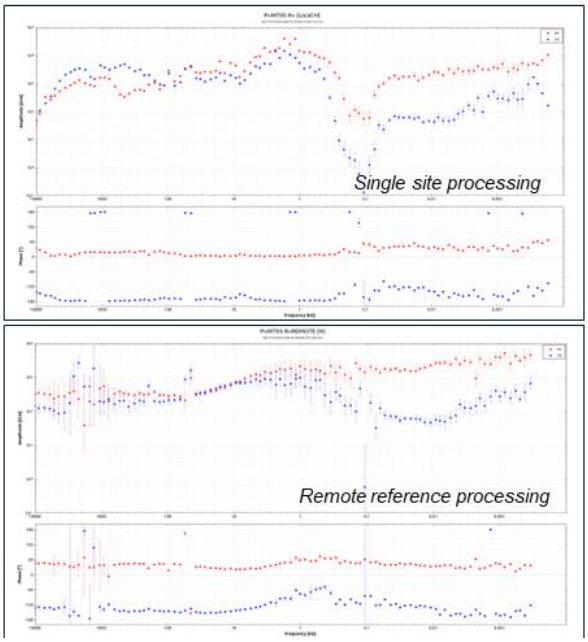

Data per site – MT02

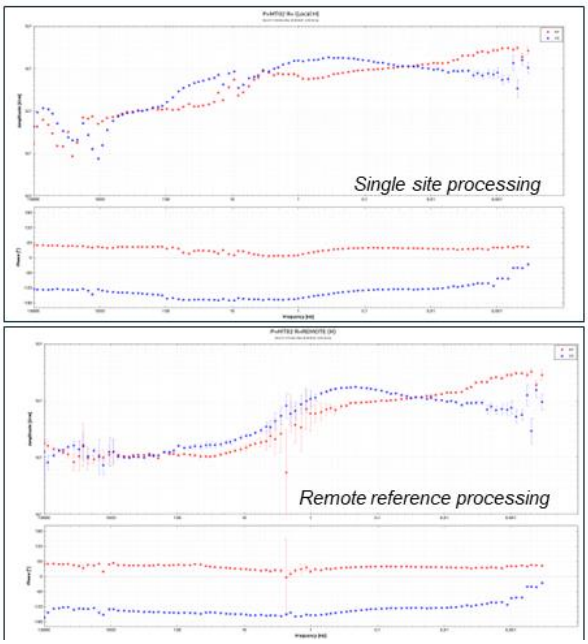

Data per site – MT01

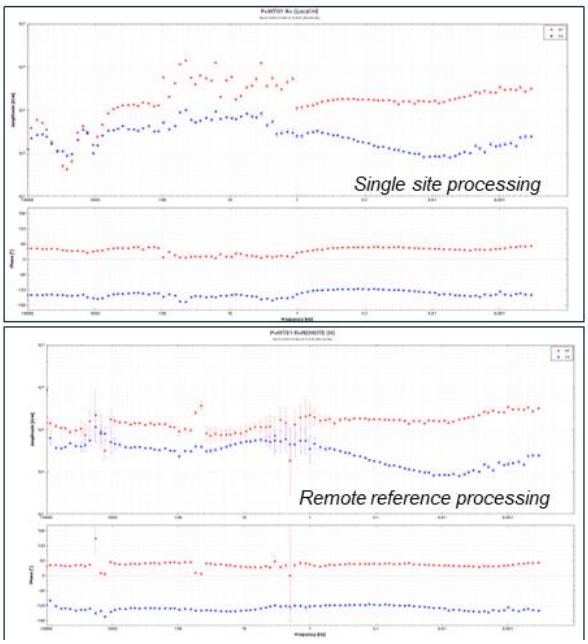

Data per site – P123

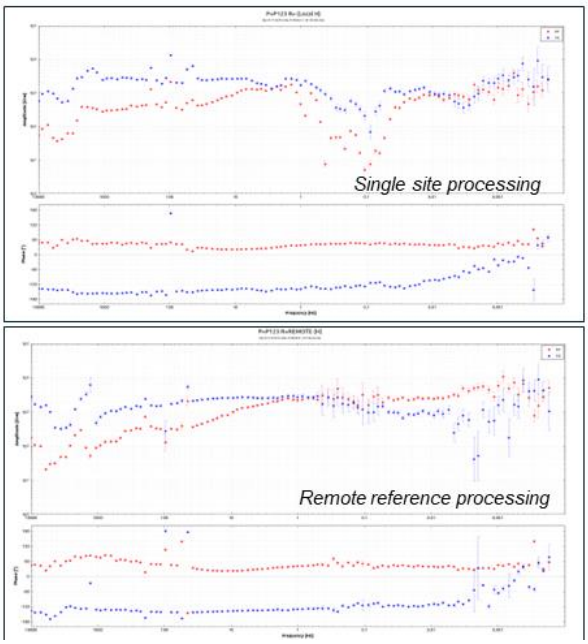

Location on field 100m close to house and local power line
Long period noise

Some improvement with remote referencing

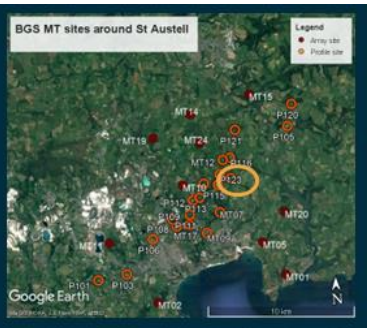

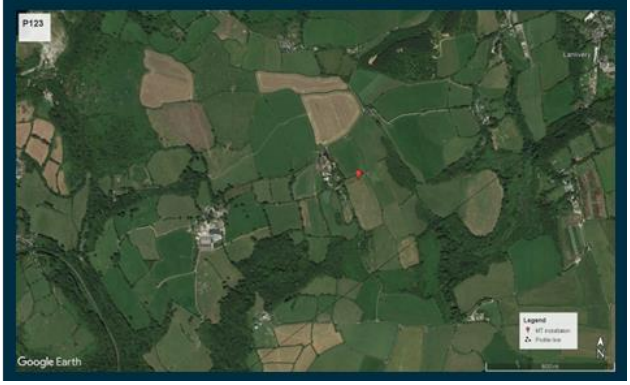

2. DATA FIT FOR PRESENTED INVERSION MODEL

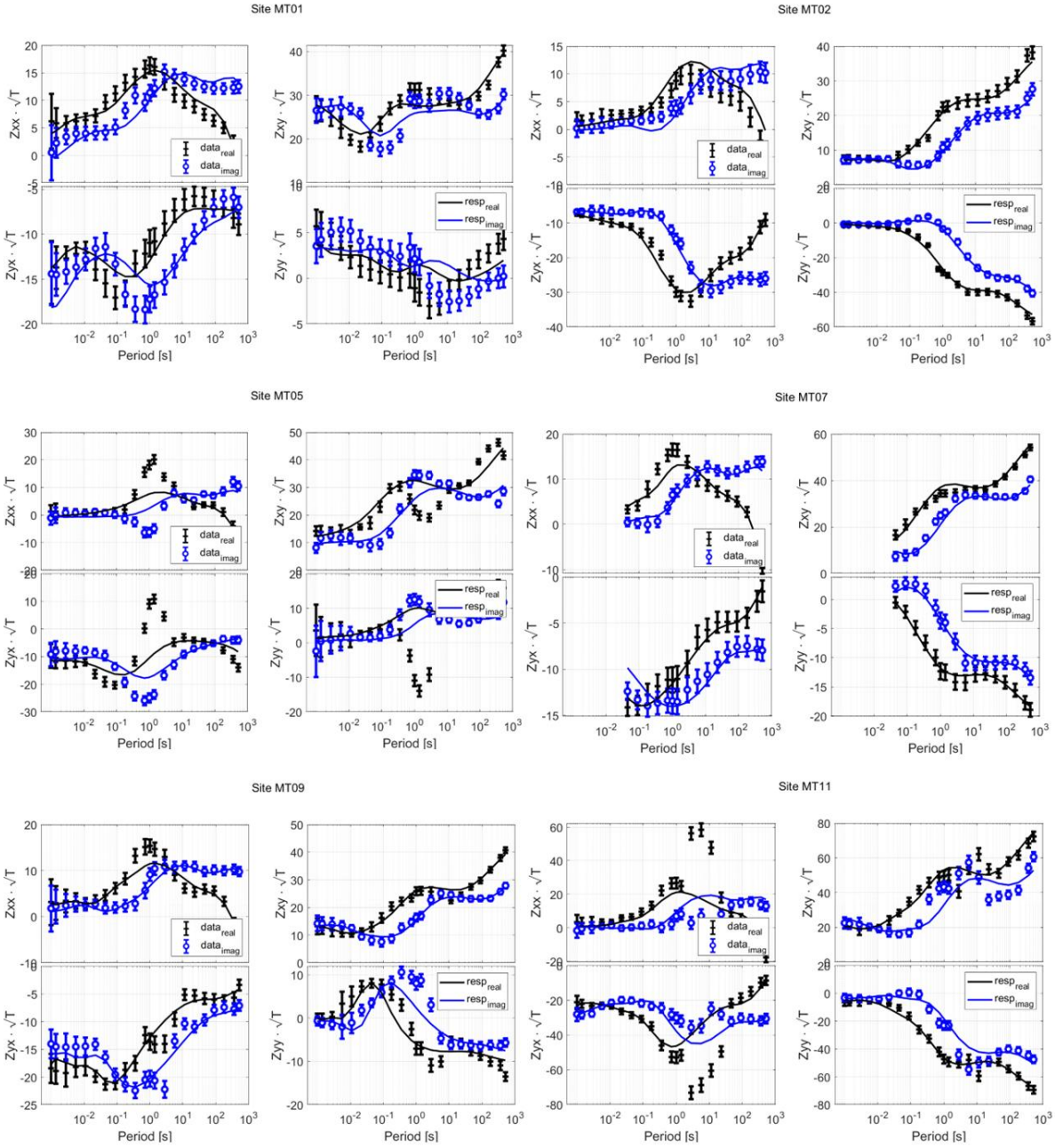

Figure 14: Data fit for presented model for sites: MT01, MT02, MT05, MT07, MT09, MT11. Four panels per site show data (circles/triangles with error bars) and forward response of the presented model (lines) for all impedance components. Contains BGS © Data UKRI 2023. All Rights Reserved.

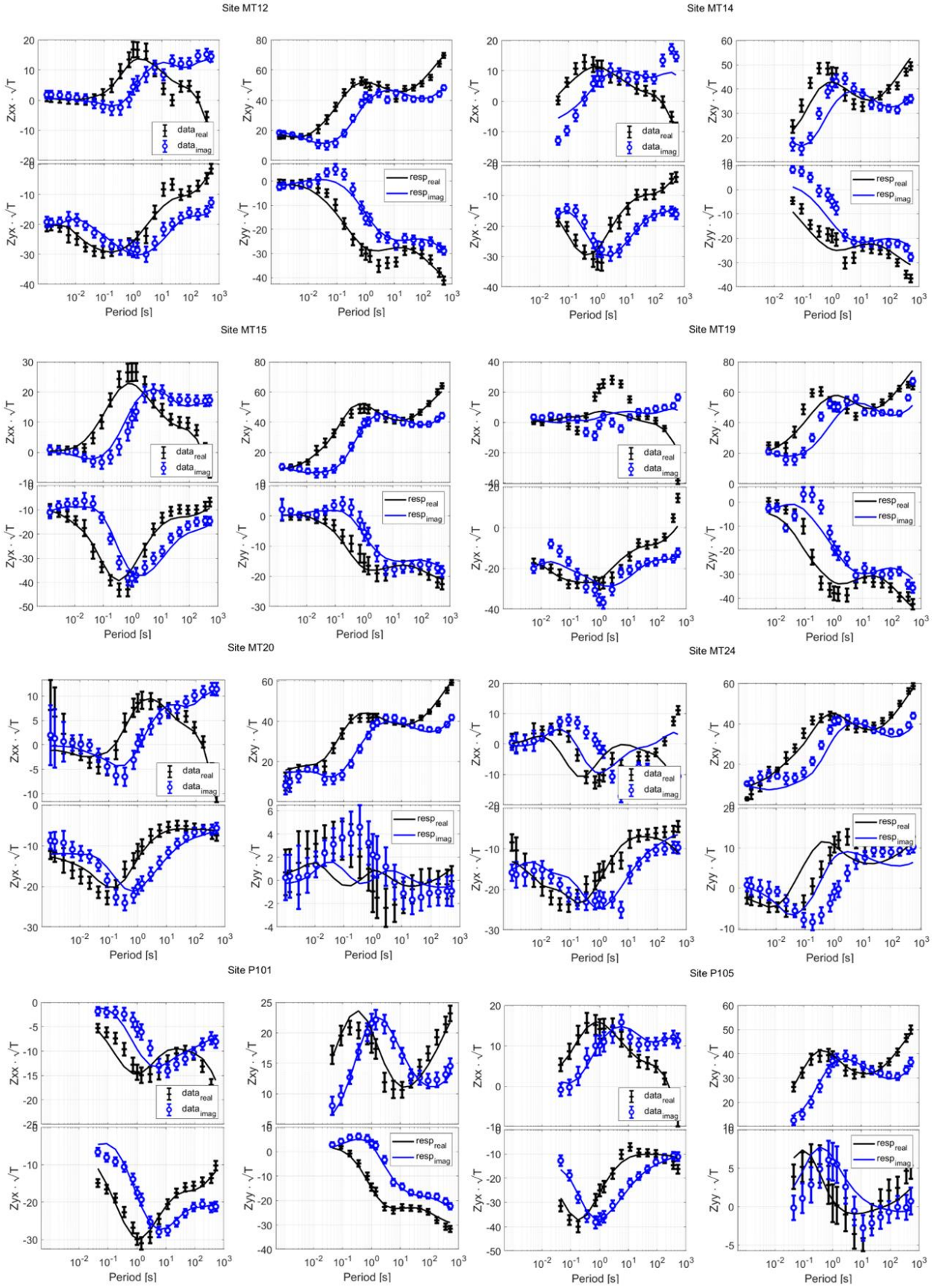

Figure 15: Data fit for presented model for sites MT12, MT14, MT15, MT19, MT19, MT20, MT24, P101 and P105. Four panels per site show data (circles/triangles with error bars) and forward response of the presented model (lines) for all impedance components. Contains BGS © Data UKRI 2023. All Rights Reserved.

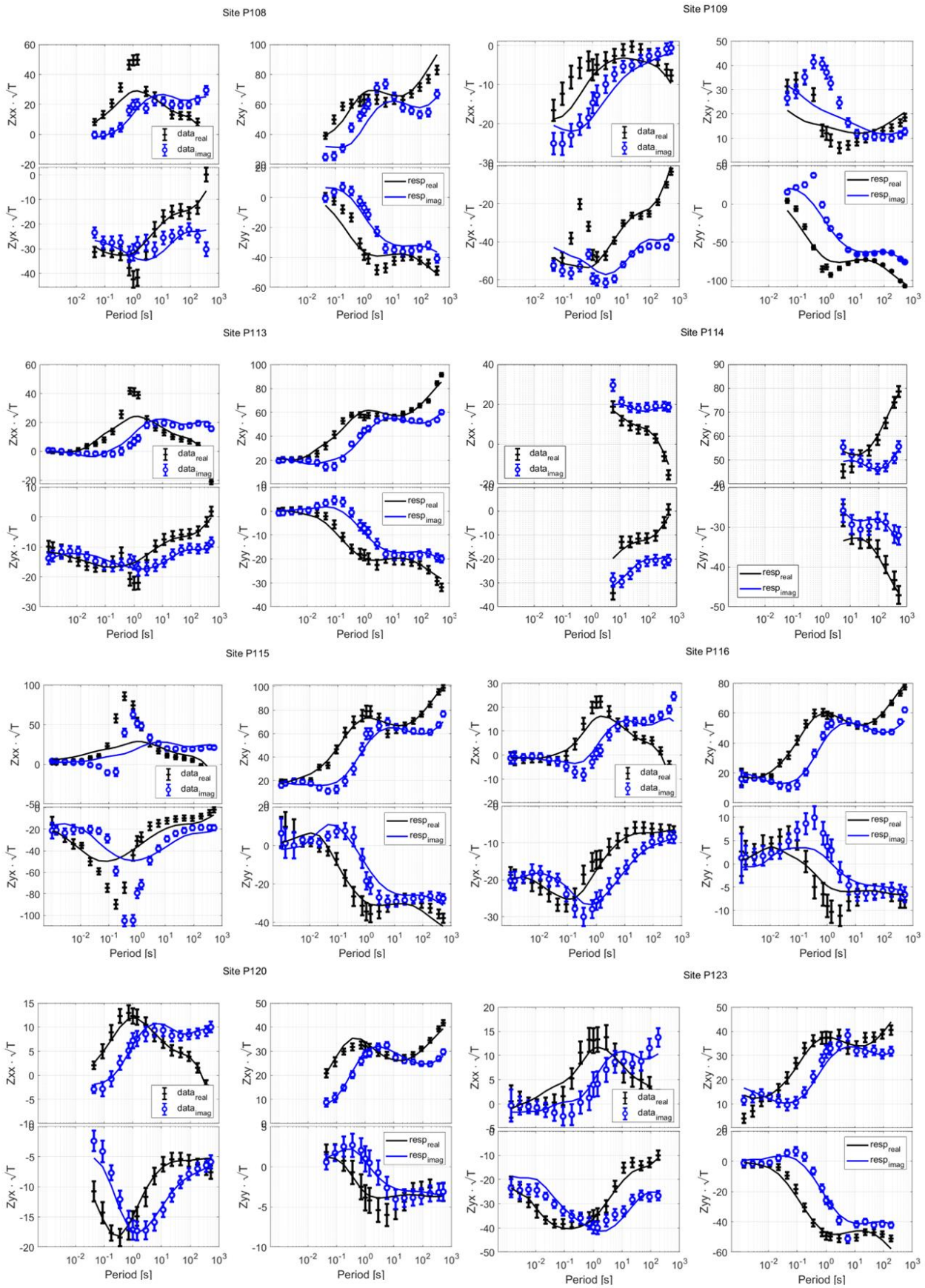

Figure 16: Data fit for presented model for sites P108, P109, P113, P114, P115, P116, P120 and P123. Four panels per site show data (circles/triangles with error bars) and forward response of the presented model (lines) for all impedance components.

Glossary

Electrical conductivity – a material property that quantifies the ability to carry an electric current. Its SI unit is S/m (Siemens per metre).

Electrical resistivity - the inverse of electrical conductivity, expressed in Ωm (Ohm metres).

EM induction – Electromagnetic induction, describing the connected effects and interaction of time-varying electric and magnetic fields.

Magnetotelluric (MT) method - passive geophysical deep-sounding techniques. MT uses simultaneous measurements of the natural variations in the electric and magnetic field at the Earth's surface to image the conductivity distribution in the subsurface.

Magnetotelluric (MT) impedance tensor – transfer function between horizontal magnetic and electric field changes under a plane-wave assumption. The tensor is frequency dependent and complex (i.e., contains an imaginary component).

References

Beamish, D., and J. Busby (2016), The Cornubian geothermal province: heat production and flow in SW England: estimates from boreholes and airborne gamma-ray measurements, *Geothermal Energy*, *4*(1), 4.

Busby, J., and R. Terrington (2017), Assessment of the resource base for engineered geothermal systems in Great Britain, *Geothermal Energy*, *5*(1).

Chave, A., & Jones, A. (Eds.) (2012), *The Magnetotelluric Method: Theory and Practice*, Cambridge: Cambridge University Press.

Gamble, T. D., J. Clarke, and W. M. Goubau (1979), Magnetotellurics with a remote magnetic reference, *Geophysics*, *44*(1), 53-68.

Huebert, J., E. Eaton., C.D. Beggan (2022), Developing a UK new ground electric field model for SWIMMR N4 (SAGE) : interim report, *Rep. OR22_067*, British Geological Survey.

Jones, P. (1992), An Electromagnetic Induction Study of South Cornwall, England, University of Edinburgh.

Kelbert, A., N. Meqbel, G. D. Egbert, and K. Tandon (2014), ModEM: A modular system for inversion of electromagnetic geophysical data, *Computers & Geosciences*, *66*, 40-53.

Munoz, G. (2014), Exploring for Geothermal Resources with Electromagnetic Methods, *Surveys in Geophysics*, *35*(1), 101-122.

Paulillo, A., L. Cotton, R. Law, A. Striolo, and P. Lettieri (2020), Geothermal energy in the UK: The life-cycle environmental impacts of electricity production from the United Downs Deep Geothermal Power project, *Journal of Cleaner Production*, *249*.

Reinecker, J., J. Gutmanis, A. Foxford, L. Cotton, C. Dalby, and R. Law (2021), Geothermal exploration and reservoir modelling of the United Downs deep geothermal project, Cornwall (UK), *Geothermics*, *97*.

Robertson, K., S. Thiel, and N. Meqbel (2020), Quality over quantity: on workflow and model space exploration of 3D inversion of MT data, *Earth Planets and Space*, *72*(1).

Tripaldi, S. (2020), Electrical signatures of a permeable zone in carbonates hosting local geothermal manifestations: insights for the deep fluid flow in the Gargano area (south-eastern Italy), *Bollettino Di Geofisica Teorica Ed Applicata*, *61*(2), 219-232.

Tschirhart, V., M. Colpron, J. Craven, F. H. Ghalati, R. J. Enkin, and S. E. Grasby (2022), Geothermal Exploration in the Burwash Landing Region, Canada, Using Three-Dimensional Inversion of Passive Electromagnetic Data, *Remote Sensing*, *14*(23).

Vozar, J., A. G. Jones, J. Campanya, C. Yeomans, M. R. Muller, and R. Pasquali (2020), A geothermal aquifer in the dilation zones on the southern margin of the Dublin Basin, *Geophysical Journal International*, *220*(3), 1717-1734.